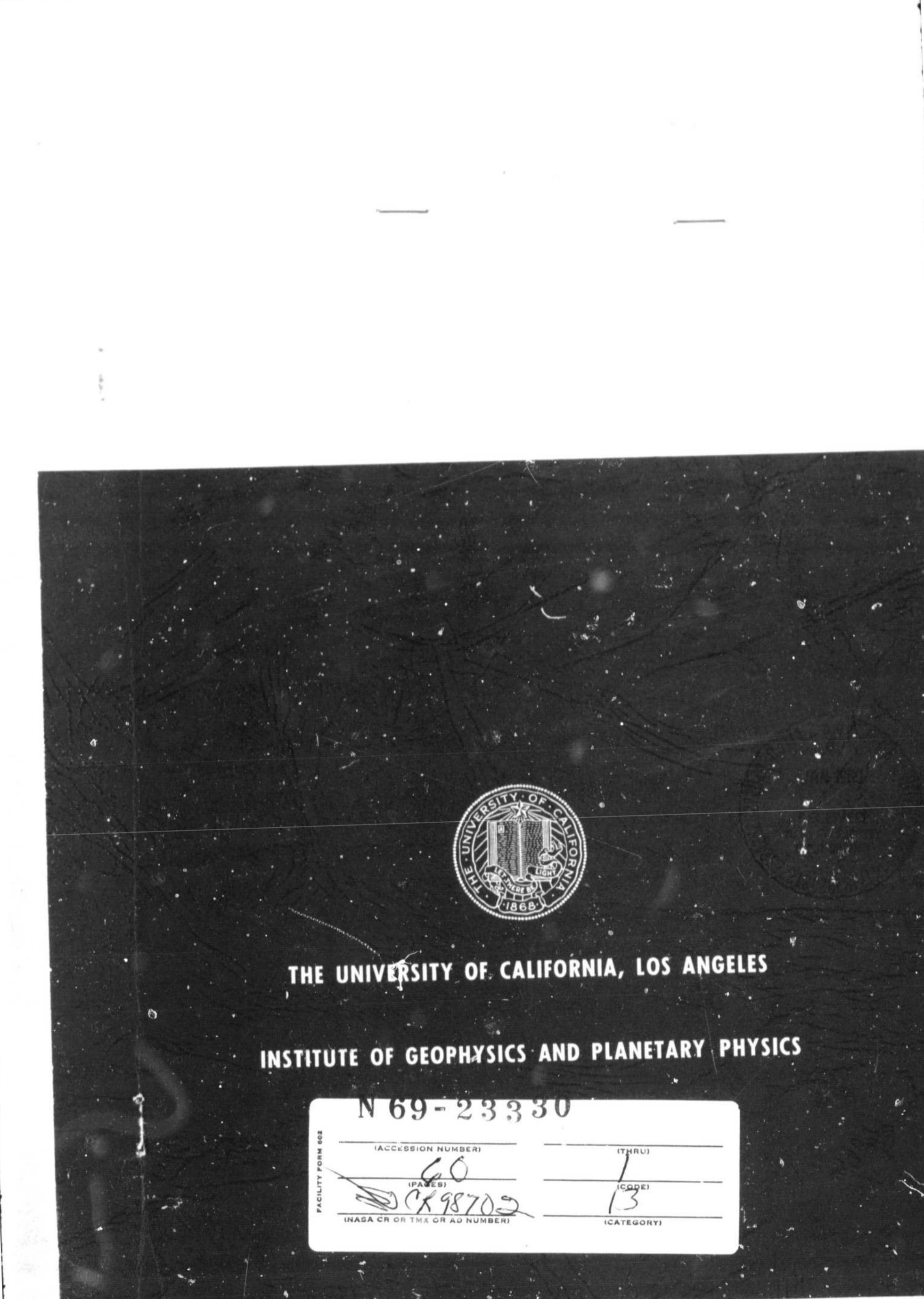

THE UNIVERSITY OF CALIFORNIA, LOS ANGELES

INSTITUTE OF GEOPHYSICS AND PLANETARY PHYSICS

OGO-3 OBSERVATIONS OF ELF NOISE IN THE MAGNETOSPHERE: PART 1. SPATIAL EXTENT AND FREQUENCY OF OCCURRENCE

Christopher T. Russell, Robert E. Holzer
(Institute of Geophysics and Planetary Physics,
University of California, Los Angeles)

and

Edward J. Smith (Jet Propulsion Laboratory,
California Institute of Technology,
Pasadena)

OGO-3 OBSERVATIONS OF ELF NOISE IN THE MAGNETOSPHERE: PART I. SPATIAL EXTENT AND FREQUENCY OF OCCURRENCE

ABSTRACT:

The magnetic noise in the magnetosphere in the frequency range from 10 to 800 hz has been extensively measured by the spectrum analyzers of the search coil magnetometer on OGO-3. This paper is a statistical study of the spatial extent and frequency of occurrence of noise at the higher end of this passband, at which frequencies, noise above the detector thresholds is most common within the magnetosphere. Steady noise and noise bursts are found to constitute two distinct populations. Both the local time and magnetic latitude distribution of both classes of signals are investigated. When the magnetic latitude distributions are extrapolated downward to 1000 km altitudes the results are consistent with previous satellite observations at these low altitudes. However, the equatorial distributions cannot be inferred by simply projecting the magnetic noise measured at low altitudes onto the equator along flux tubes.

The in situ measurements cannot determine the exact location of the source of all the noise observed. However it is found that steady noise is definitely generated near 45 degrees magnetic latitude on the dayside of the magnetosphere for L-values from 6 to 10 and that bursts are generated near the equator above L=8 from 0400 to 1800 local time. The latter observation can be used to explain the generation of both auroral microbursts and chorus as seen on the ground via whistler mode wave growth at the equator supported by a pitch angle anisotropy maintained by the loss cone.

OGO-3 OBSERVATIONS OF ELF NOISE IN THE MAGNETOSPHERE: PART 1. SPATIAL EXTENT AND FREQUENCY OF OCCURRENCE

Christopher T. Russell, Robert E. Holzer
(Institute of Geophysics and Planetary Physics,
University of California, Los Angeles)

and

Edward J. Smith (Jet Propulsion Laboratory,
California Institute of Technology,
Pasadena)

INTRODUCTION:

Previous observations of ELF noise in the magnetosphere have been made at low altitude (Gurnett and O'Brien, 1964; Taylor and Gurnett, 1968; Oliven and Gurnett, 1968). Such measurements made near the lower magnetospheric boundary are not necessarily representative of the distribution of signals throughout the entire magnetosphere because ELF signals generated near the magnetic equator may never penetrate to low altitudes due either to reflection or absorption, or both (Thorne and Kennel, 1967; Kennel and Thorne, 1967). In addition signals may not be entirely guided along field lines. The purpose of this paper is to give the character of the signals measured in situ in a wide range of positions within the magnetosphere, covering all local times, most L-shells out to the magnetopause on the front of the magnetosphere, to the tail at the rear, and at many magnetic latitudes.

Section 1 of the paper is devoted to a description of the triaxial search coil magnetometer used for the measurements and to relevant details of the spacecraft and orbit.

Section 2 is a description of the methods of analysis used to organize the data, including a discussion of interference. The distribution of magnetic noise in local time - L-value space is presented and discussed in Section 3. The distributions of noise in magnetic latitude averaged over certain sectors of local time and L-values is given in Section 4. Finally, the location of the most probable regions of noise generation and a possible mechanism for the generation of magnetic noise are discussed.

1.1 INSTRUMENT:

The instrument is essentially the same as the search coil magnetometer carried on board OGO-1, some details of which have been described by Holzer et al. (1966) and Smith et al. (1967). Some of these details will be repeated here to give a coherent description of the overall experiment. Not all the details of the instrument will be relevant to this paper, however, but will bear on later papers of this series.

The instrument consists of three orthogonal search coils, each containing 100,000 turns of copper wire wound around a permeable core. The voltage output of the coils is proportional to the frequency of the magnetic fluctuation to about 700 hz. Thereafter, the response of the coils rolls off as shown schematically in graph a) of Figure 1b. The coils arbitrarily designated as the X, Y, and Z-axis, are mounted at the end of a 20 foot boom to isolate the experiment from spacecraft fields.

The signals from each coil caused by the fluctuating magnetic fields are amplified a factor of 100 before being transmitted down the boom to the main electronics package situated in the body of the spacecraft. A block diagram of the circuits for a single sensor is shown in Figure 1a. The circuitry is repeated for the outputs of each of the three orthogonal coils and the outputs are independent except as related by the projections of the perturbation field on each of the three coils. The signals from each sensor are passed through a rejection filter centered at 400 hz to eliminate the strong spacecraft power frequency. The passband of this filter which also rejects signals above 1200 hz is shown in graph b) of Figure 1b. Then the signals are divided into two paths, the waveform channel and the spectrum analyzer channel.

The waveform channel filters the signals with both high pass and low pass filters. The high pass filter has a 9 db point of .004 hz and an attenuation of 18 db per octave. The low pass filter has a corner frequency of 0.8 hz when the satellite transmits data at the two lowest rates and a corner frequency of 70 hz when the satellite transmits data at the highest data rate. The low pass filter has an attenuation of 12 db per octave. This is illustrated by graph d) of Figure 1b.

As indicated in Figure 1 the waveform channel also has a variable gain. The total gain from coil to waveform channel output can be either 700, 7000 or 70,000 on command from the ground. This combined with a coil constant of

10 μv/γ-hz means that a signal oscillating at 1 hz with an amplitude of 1 γ will produce an output voltage of 0.7 volts in the highest gain state. The telemetered output of the experiment can range from 0 to 5 volts. The waveform channel outputs have a resting level of 2.5 volts so that changes in signal polarity may be determined. All outputs are digitized into 255 steps, each with a width of approximately .02 volts. The spacecraft telemeters the data at one of three bit rates 1,000, 8,000 or 64,000 bits per second. One word requires nine bits (one for parity) and since the spacecraft telemetry system samples the output of all the experiments in a 128 word cycle, the experiment cycle is completed in either 1.152, 0.144, or 0.018 seconds. Each coil's waveform channel has 5 of these 128 words almost evenly spaced in time giving rise to Nyquist frequencies of 2.2, 17 or 139 hz depending on the telemetry bit rate.

The other path that the signals take is called the spectrum analyzer channel. Here, the signals are amplified and passed through five parallel filters centered at 10, 30, 100, 300 and 800 hz. The filters are each 20 db down at the adjacent center frequency and ~ 6 db down at geometric mean. This is illustrated in graph c) of Figure 1b. These five filters are each followed by peak detectors with a rise time of one second and a decay time of about 40 seconds. The long decay time provides a primitive data storage device as 14 outputs of the spectrum analyzer channel are sampled by the spacecraft subcommutator which completes one cycle every 128 of the above main cycles. During the

subcommutator cycle some of the channels are sampled once, some twice and others three times. The output of the filter on the Z-axis coil centered at 10 hz is sampled once in every cycle of the main commutator, that is, every 1.152, 0.144 or 0.018 seconds. The gain of the spectrum analyzer channel may also be in a low, medium or high state which differ by factors of 10 and is changed by ground command.

Except when the signals rise faster than one second or fall faster than 40 seconds the signals returned by the 15 outputs of the spectrum analyzer channel are thus slowly varying DC signals proportional to the square root of the power present in bands around logarithmically spaced center frequencies.

The amplitude obtained after the spectrum channel filters from a monochromatic signal into the coils, i.e. a pure sinusoidal tone, depends upon the frequency, of course, because of the response of the coil and upon the gain of the filter but also upon the distance in frequency of the tone from the center frequency of the filter. If the signal is not a tone but a broad band spectrum of signals across the bandwidth of the filter there is a different constant of proportionality dependent upon the spectral shape of the noise. Table 1 lists the amplitude of the monochromatic tone which would give rise to one volt output from each of the spectrum analyzers if it were at the center frequency of that filter. It also lists the spectral power density of white noise (spectral power density constant across the

filter bandwidth) and the spectral power density of pink noise (spectral power density varying inversely as the square of the frequency across the filter bandwidth) which would result in one volt output from each of the spectrum analyzers.

It can be seen from Table I that an exact measurement of the amplitudes of the observed signals depends somewhat on a knowledge of the spectral characteristics of the signals. In the following analysis all data will be given in observed voltages and it will be assumed that all signals of a given population (steady noise or bursts) have similar spectral characteristics.

We also note that if one knows that a signal is monochromatic, we can estimate its frequency from the ratio of the amplitudes of the outputs of the two filters that bracket the tone. Thus we can estimate frequencies using the spectrum channel outputs alone for monochromatic tones between 10 and 800 hz.

1.2 SPACECRAFT AND ORBIT:

The spacecraft and mission of the OGO satellites have been previously described by Ludwig (1963). Several pertinent details will be included here. The spacecraft was launched from Cape Kennedy on June 7, 1966. It was designed to have three-axis stabilization in a known orientation utilizing a system of reaction wheels and gas jets. This was achieved for the first twenty-three orbits. Thereafter the spacecraft was spin-stabilized with a spin-period of about 100 seconds. Sufficient gas was available to change

spin-axis orientation when power requirements demanded and to maintain the spin-period.

Perigee was at an altitude of about 250 km and apogee at 20.2 earth radii geocentric. The resulting period was 2 days and 33 minutes. The spacecraft completely swept out the two dimensional space defined by local time and L-value within the magnetosphere in the first year of operation with relatively few intervals of lack of data.

While the satellite was inertially stabilized some estimate of the polarization of the fluctuating field could be made from the relative amplitudes of the outputs from three spectrum analyzers at one frequency on the three orthogonal coils. These studies will be reported in a later paper of this series. However, during the spin stabilized mode of operation this calculation was severely complicated.

1.3 INTERFERENCE:

Measurements of fluctuating fields in space are often subject to sources of signal other than those which the experiment intended to measure. These may come from the spacecraft itself or from the other experiments. On a spacecraft as sophisticated as an OGO or with as many experiments (20) one must be cautious in interpreting results. Clues as to whether a signal is "real" or is "interference" can be obtained from whether the relative amplitudes of the fluctuations change on different coils as the coil orientation changes relative to the field; whether a precise frequency is observed independent of

external conditions such as field strength and position in space; whether the signal characteristics such as duration or amplitude are exactly repeated on each observation; whether signals repeat at very regular time intervals; whether the signals correlate with spacecraft functions that are monitored or with the times of commands; etc.

Although computers were used in the analysis, all of the data reported here were scanned visually in amplitude versus time plots and the above criteria were used to reject all intervals in which interference could be detected. In all, about 25% of the data was rejected and it is believed that a negligible fraction of the data remaining is affected by interference.

2. ANALYSIS:

For the study of the occurrence of signals within the magnetosphere, the signals were arbitrarily divided into two categories: steady signals and bursts of signals. Steady signals were those which persisted or changed slowly on the 100, 300 or 800 hz spectrum channel over a period longer than two minutes. When the satellite was spin stabilized this was usually equivalent to saying that the spin induced modulation of the amplitude dominated over changes in the signal strength. The 100, 300, and 800 hz channels were picked because an initial study showed that within the magnetosphere, these outputs contained the dominant activity. Signals at other frequencies are present but much less frequently. The occurrence of these signals is

important also but a report on their occurrence will be deferred to a later paper.

Bursts meant that the signals rose and fell in a period of time less than two minutes and reached a level of greater than two volts on either the 30, 100, 300 or 800 hz channel. The majority of bursts, however, had a rise time of much less than a minute. Usually the rise time was several seconds or less. When the satellite was spin stabilized this category was characterized by changes in signal strength dominating over the modulation induced by the spin. The two categories are not mutually exclusive. Both steady signal and bursts were noted on occasion simultaneously. However on those occasions when the steady signal was strong enough to saturate the telemetry capability of 5 volts no bursts could be observed or when bursts occurred so frequently that the level of the detectors could not decay sufficiently between bursts, then steady signal could not be detected. Figure 2a shows an example of steady noise occurring while the satellite was inertially stabilized. Here the raw outputs of each of the five analyzers on each of the three axes are plotted versus time in hours and minutes. The marks on the vertical axis represent the zero level of each detector and the distance between closest marks represents full scale or five volts. At this time the signals are strongest on the 300 and 800 hz outputs and stronger along the Z coil than the X and Y. In fact the signals occasionally saturate the Z300 and Z800 outputs. The signals strength at 100 hz is much less and the 30 and 10 hz analyzers are at

their resting levels. These data were taken at a local time of 1530, an L-value of 4.0 and a magnetic latitude of 29° and the Kp index was 1^+.

Figure 2b illustrates steady noise occurring while the satellite was spin stabilized. The scales of Figure 2a apply. The spin period is the time interval between maxima on the X and Y-coil outputs. The modulation on the Z-coil is at twice the spin frequency. This occurs because the Z-coil is almost exactly perpendicular to the spin axis of the spacecraft and will see the same signal amplitude upon rotation of 180 degrees. The other two coils have a component along the spin axis and one perpendicular to it and are not in an equivalent position upon rotating 180 degrees. Here the steady signal is seen only on the 100 and 300 hz analyzers. These data were taken at a local time of 1640, an L-value of 3.9 and a magnetic latitude of 7.5°. The Kp index was 3^-.

Figure 2c illustrates what we have categorized as a slow burst of noise with data taken while the satellite was inertially stabilized. The scales of Figure 2a apply. This type of data is not common. The local time here was 1740, the L-value 6.3, the magnetic latitude 23°, and the Kp index 1^+.

Figure 2d shows rapid bursts of signals obtained while the satellite was spin stabilized. The scales of Figure 2a apply except that these data were obtained in the medium gain state and hence a signal must be 10 times stronger to

cause saturation than it was in previous examples. The local time here was 1410, the L-value 8.2, the magnetic latitude 1.7° and the Kp index 3⁻.

In the study reported here raw data plots of the spectrum analyzer outputs in the format presented in Figure 2 were scanned visually for all the data available from OGO-3 at the two highest data rates for orbits 1 to 202, that is over a span of one year and 44 days. Data recorded at the lowest bit rate were not used because of the possibility of missing bursts of noise due to the low sampling rate. The type of signal present was recorded for each five minute segment of data. If the satellite was close to perigee and changed position rapidly or if the amount of continuous data were not a multiple of 5 minutes, occasional segments of data less than 5 minutes were used. If steady signals were present at one or more frequencies an amplitude in volts was recorded at each frequency averaged over the interval. If one or more bursts occurred at any frequency during this interval only the fact that bursts were present was noted. The number of bursts during this segment of data was not recorded. The orbit number, L-value, local time, magnetic latitude and duration of each segment of data were also noted. These facts were put on punch cards to permit sorting by L-value, local time, or magnetic latitude. The percentage of the time that steady signals and bursts were observed in various positions within the magnetosphere were calculated as well as the length of time spent in that location and the number of different orbits used in the average. Since the

orbital period is over two days, the number of different orbits is roughly a measure of the independence of the samples used in the average, assuming magnetic activity has a scale time of two days or less.

Even though the difference between the calculated L-value and actual equatorial distance of a field line increases as L increases and in fact is very large near the magnetopause, L-values up to 12 were used because it was felt that in dealing with phenomena, that may be contained by the field, an incorrect L-value would order the data better than radial distance.

Within an L-value of 12 for the first 202 orbits there were 32,241 minutes of interference free data at various magnetic latitudes, in no way distributed uniformly throughout the magnetosphere. Of this, 24,136 minutes were within magnetic latitude $\pm 30^{o}$, and were used to construct the equatorial local time distribution of the observed signals.

3.1 LOCAL TIME DISTRIBUTION:

The data within $\pm 30^{o}$ magnetic latitude were first sorted by L-value and local time into boxes of dimension one earth radius by one hour for L-values greater than 5 and into boxes of dimension one earth radius by two hours local time for L-value less than 5. The percentage of the time within each box that either the 100 hz or 300 hz channel was above 1 volt or the 800 hz channel above 2 volts was calculated and is presented in Figure 3. Blanks occur when data were not available or when data from only one

orbit were available. This figure shows that steady signals are most common on the dayside of the magnetosphere within L=6 and on the nightside within L=5, and that within these L-values steady signals are more common on the dayside than the nightside.

The same data are presented in Figure 4 except for signals of greater than 4 volts on the 100, 300 or 800 hz channels. This plot shows a reduction in the frequency of occurrence of steady signals in all regions and it shows a marked day-night asymmetry. This implies that the signals seen on the dayside are on the average stronger than those seen on the nightside.

Figure 5 shows the occurrence of bursts in the same format as the previous two figures. The most obvious feature is the lack of bursts in the dusk to midnight quadrant. In fact, most of the bursts occur between the hours of 0400 and 1600. Also, most bursts occur beyond L=5.

3.2 DISCUSSION:

The distributions of signals observed near the equatorial plane as displayed in figures 3, 4, and 5 are similar in some respects and dissimilar in other respects to the distributions obtained by Injun III at low altitudes (Gurnett and O'Brien, 1964; Taylor and Gurnett, 1968; Oliven and Gurnett, 1968). The Injun III data have been divided into two broad categories: hiss and chorus (Gurnett and O'Brien, 1964). These categories bear some resemblance to but are not necessarily congruent with the categories used for the OGO-3 data.

The digital data transmitted by Injun III records the minimum signal seen between samples which are generally two seconds apart. Impulsive noise or signals consisting of fine structure which lasts less than two seconds will not be recorded and therefore noise distributions obtained from the digital data will be representative of hiss rather than chorus or whistlers. The chorus is identified by the analog telemetry of the experiment which permits a reconstruction of the frequency-time characteristics of the signals.

On the other hand, our analysis requires noise to be at a near constant level for two minutes to be classified as steady noise. In addition, if the fine structure in chorus were closely spaced and fairly constant in amplitude for several minutes and rise and decay times of our instrument would give the appearance of steady signal. However, this is considered to be a rare occurrence and we expect, in fact, that in our analysis most chorus is classified as data containing bursts. Besides chorus we would also count whistlers and hiss variations on a time scale of less than two minutes as bursts.

The analysis of chorus on Injun III by Oliven and Gurnett (1968) shows chorus occurring mainly from 0400 to 1300 LT with some chorus as early as midnight and as late as 1800. In addition chorus is seen on L-shells as low as 2 and as high as 15. The distribution of chorus in local time then agrees with the distribution of bursts on high L-shells. However, the occurrence of bursts decreases as

we move into lower L-values even where the occurrence of chorus as observed by Injun III is large. We attribute this to the fact that the Injun III data extend to higher frequencies and the bursts at lower L-values are at frequencies above our passband. In fact an increase in the center frequency of bursts as the satellite moves to lower L-values is observed in the region beyond L=6. The bursts that we do see at low L-values and which do not have the same local time dependence as the chorus are probably due to whistlers and variations of the hiss in periods of less than two minutes. In fact, we expect more whistlers at low L-values than at high L-values (Carpenter et al., 1968).

In the paper by Taylor and Gurnett (1968) the local time distribution of noise recorded by the digital system is presented. In the frequency range from 700 to 7000 hz the steady noise, or hiss occurs almost exclusively on the dayside of the magnetosphere. It also rarely occurs lower than an L-value of 3, but extends to L-values greater than 15. This is to be contrasted with our results that show the steady noise near the equator to be confined mainly to L-values below 4 and only a weak day-night asymmetry. This again could be due to the differing passbands of the two experiments but could also be due to the distribution of the noise down the field line. In the next section we investigate this distribution.

4.1 MAGNETIC LATITUDE DISTRIBUTION:

Dividing the data as presented in figures 3, 4, and 5 further by magnetic latitude would introduce large variations from region to region due to statistical variations alone. In addition the satellite does not sweep through an entire magnetic latitude range at a specific local time and L-value. Thus in dividing the data up by magnetic latitude we have averaged over sometimes rather large areas in local time, L-value space, trying not to mask out any changes in the distributions from one position to the other. In addition we have not attempted to divide the data which were taken below L=2 by magnetic latitude. The data here are very sparse and in addition not well distributed in magnetic latitude.

Figures 6a, b, c, d show the distributions of steady signals and bursts for the local times from 0900 to 1800 at various L-shells. The threshold for detection of steady signals for these and the following magnetic latitude distributions is the same as that for Figure 3, that is greater than 1 volt on the 100 or 300 hz channel or greater than 2 volts on the 800 hz channel. The threshold for the detection of bursts is 2 volts on either the 30, 100, 300 or 800 hz channel. The solid black bars indicate the percentage occurrence of bursts in each 10 degree range of magnetic latitude and the cross-hatched bars indicate the percentage occurrence of steady signal in the same 10 degree range. The total time, T, in minutes, spent in each 10 degree range is

indicated along with the number of orbits, N, and also the average magnetic latitude, λ, of the samples used.

In the discussion to follow we shall refer to the distributions of Figure 6 as the dayside distributions even though the period from 0600-0900 LT is also above the sunlit hemisphere. The reason for this is that the period from 0600-0900 LT does not show the same characteristics in the distribution of steady noise as the rest of the dayside magnetosphere and may be a region of transition from night-time characteristics to day-time characteristics.

Within L=5 the occurrence of steady signals is quite high at all magnetic latitudes, and the occurrence of bursts is small. Beyond L=5 the occurrence of steady signals at low latitudes decreases but the occurrence rate at high latitudes remains quite high. Between L=5 and L=6 this region of frequent occurrence of steady noise spans magnetic latitudes from 30 to greater than 50 degrees. However as we proceed outwards this region narrows so that in the range from L=8 to L=9 it spans only the latitudes from 40 to 50 degrees. We note that here the occurrence of steady magnetic noise decreases both to lower and to higher magnetic latitudes. At L-values above 9, the occurrence rate at high latitudes decreases and seems to move to lower latitudes.

On the other hand bursts become more frequent beyond L=5. Two general trends are evident. As we move outwards along a line of constant magnetic latitude bursts become more common and as we move away from the equator along an L-shell to higher magnetic latitudes bursts become less

common. The apparent violation of this trend between L=8 and L=10 for magnetic latitudes between 10 and 20 degrees is due to a large contribution of time from two consecutive quiet orbits to these two points. The enhancement at high magnetic latitudes for L-values between 5 and 7 appears to be more than a statistical fluctuation, but the bursts counted here may be due to a different source than those with the characteristics described above.

Figure 7 shows the night-time distributions below L=6. The occurrence of steady signals is less common than on the dayside as shown in Figure 6a and the occurrence of bursts somewhat more common. The post-midnight distributions are fairly uniform with magnetic latitude except for an enhancement of steady signals near the equator. The pre-midnight distribution of steady noise shows a weak enhancement around 30^{o} and the bursts are more common at magnetic latitudes above 40^{o}.

Figure 8 shows the night-time data between L=6 and L=8. The post-midnight sector extends to 0900 LT because the data from 0600-0900 LT exhibited the same behavior as the data from 0000-0600. We see that steady signals rarely occur in either sector and that bursts are common only in the post-midnight sector. In addition the bursts occur less frequently as we go to higher magnetic latitudes in this sector. This is the same effect as we saw in figures 6b, c, d on the dayside.

Figure 9 shows the post-midnight and pre-midnight

sectors for L-values between 8 and 12. The post-midnight sector has been shortened to include only 0000-0400 LT because of a change in the occurrence of bursts after 0400. In both sectors steady signals are rare. Bursts are more common than the steady signals but on the other hand less common than in the same local time sectors at lower L-values.

Figure 10 shows the distributions in the remaining two regions of the magnetosphere. The lower histogram shows the distribution for local time between 0400 and 0900 for L-values between 8 and 12. Here steady signals are rare, as they were from 0000-0400 and from 1800-2400 LT in Figure 9. However, bursts are much more frequent and occur with a frequency similar to that shown in Figure 6d for local times from 0900-1800. Again, the trend for a decreased occurrence rate away from the equator is evident.

The upper histograms of Figure 10 show the region below L=6 from 0600-0900 LT. Here steady signals occur more frequently than from 0000-0600 but less frequently than from 0900-1800. The distribution of steady signals is also fairly uniform with magnetic latitude but no data were obtained near the equator here. Bursts are not common at low latitudes. However there is an increase in the number of bursts with increasing magnetic latitude so that bursts are quite common between 40 and 50 degrees. The lack of bursts above 50^{o} may be a statistical fluctuation since we have only 6 minutes of data taken from two orbits here.

In order to facilitate a visualization of the actual distribution of noise on the dayside of the magnetosphere we have plotted in Figure 11 the distribution of steady signals from 0900-1800 of figures 6a, b, c, d slightly differently. On a grid consisting of dipole field lines and lines of magnetic latitude we have shaded each block as to frequency of occurrence. We note that the actual L-values of the data were obtained from a multipole expansion of the field. The dipole lines are used just for the graphical representation.

In the magnetic latitude distributions shown in Figure 11 an occurrence of steady signal was noted whenever the signal strength was 1 volt or more on the 100, or 300 hz channel or a signal of 2 volts or more on the 800 hz channel. If we increase our threshold for the detection of steady signals so that we are considering signals greater than 4 volts on any one of these three channels we obtain the distribution of Figure 12. This illustrates that within L=4 the signals are strongest between about 20 and 40 degrees magnetic latitude, whereas for L-values greater than 4 they are strongest between 40 and 50 degrees.

In Figure 13 we show the day-time distribution of bursts on the same type of diagram. This brings out the trend for increased burst activity as we move to higher L-values on a line of constant magnetic latitude and also the trend for decreased activity as we move to higher magnetic latitudes along an L-shell.

4.2 DISCUSSION:

Both the local time distributions and the magnetic latitude distributions indicate that the steady noise and bursts are on the average quite separate phenomena. At low L-values steady noise is quite common at all local times and except from 0000 to 0600 LT the steady noise has only a weak magnetic latitude dependence. At higher L-values, however, steady signals are only a day-time phenomenon occurring at high magnetic latitudes. Bursts are most common at high L-values, from 0400 to 1800 LT, and occur less frequently as one moves away from the equator.

We would like to use these facts to understand the mechanism for the generation of these signals, but we have to consider first what the distributions tell us about the location of the source. We will examine this question below and test a proposed mechanism,but before doing so,we will examine the discrepancies mentioned in section 3 between the Injun III local time distribution of hiss, and our observations of steady noise near the equator in light of the magnetic latitude distributions.

First, the marked day-night asymmetry observed by Injun III is a result of the fact that the high magnetic latitude steady noise is a day-time phenomenon. Second, the observation by Injun III of hiss to higher L-values than is shown in Figure 3 for magnetic latitudes within 30^{o} of the equator is explained by the fact that at high L-values the steady noise is not observed near the equator

but is present only at high magnetic latitudes. However, the lack of observations of hiss by Injun III at lower L-values where steady noise is common at all magnetic latitudes is not as obvious. Perhaps the noise is absorbed before it reaches the orbit of Injun III or perhaps the noise lies below Injun III's passband in this region. Also, it might be argued that Figure 6d indicates that the steady signals observed at high latitudes for L-values greater than 9 do not reach Injun III and hence there is still a discrepancy between the OGO-3 and Injun III results. However, we note that the signals near L=8 upon reaching Injun III's altitude do not have to propagate very far, parallel to the earth's surface, to distort the magnetospheric L-value distribution. Also, as with the discrepancy in the L-value distributions of bursts and chorus, the explanation could lie in the differing passbands of the two instruments. In light of the above, we feel that the Injun III observations agree with what one would expect upon extrapolating to low altitudes our observations made at higher altitudes while taking into account the differing passbands. This, in turn, implies that for the most part what we term to be steady noise corresponds to ELF hiss and what we term to be bursts, at high L-values, corresponds to chorus at lower altitudes.

Turning to a consideration of the location of the sources of the observed noise, we note that the location of the most frequent occurrence of signals or of the strongest

signals is not necessarily the location of the source of the signals if we have focusing of the signals as they propagate away from the source. If absorption is strong enough to damp signals before focusing becomes important, of course, the observed occurrence maximum and the source will coincide. However, assuming absorption is negligible and that signals are completely guided along the field we can get a strong focusing effect. In this case, the energy flux down the tube (the product of the group velocity, the square of the wave amplitude, and the area of the flux tube) is constant. For whistler mode propagation well below the electron gyrofrequency the group velocity is proportional to the square root of the field divided by the number density. For diffusive equilibrium along field lines which appears to be valid within the plasmapause (Angerami and Carpenter, 1966), the number density is roughly constant. This combined with the fact that the area of the flux tube is inversely proportional to the field strength, results in a wave amplitude that grows as the fourth root of the field. In the collisionless model which seems to be valid outside the plasmapause (Angerami and Carpenter, 1966), N is roughly proportional to B and the group velocity is almost constant. In this case the wave amplitude is proportional to the square root of B. Thus, at 45^{o} magnetic latitude complete guidance by field lines would give a wave amplitude of 3.6 times the equatorial amplitude for the collisionless model and 1.9 times the equatorial amplitude for the diffusive equilibrium model. The several

cases of noise distribution will be examined with this calculation in mind.

The low L-value steady noise distribution between 0000 and 0600 LT shown in Figure 7 strongly indicates that the principal noise source is near the equator and that the decrease at higher magnetic latitudes is due to absorption. However, between 1800-2400 LT the noise source might be placed anywhere from 0 to 30 degrees. Similarly, the distribution of steady noise on the dayside at low L-values is consistent with a source located almost anywhere between 0 and 40 degrees. Alternatively it is possible that the source is extended over a large range of magnetic latitudes and strong absorption is present.

The high L-value, high magnetic latitude steady noise which exhibits a maximum in the vicinity of 40^{o} in figures 6b, c, and d, cannot be explained in terms of an equatorial source plus focusing. For example, between L=7 and 8 steady signals above 1 volt on the 100 or 300 hz channel or above 2 volts on the 800 hz channel are present 8% of the time near the equator, whereas between 40 and 50 degrees, 71% of the data consists of steady noise above 4 volts. This means that 63% of the time an amplification of greater than 4 is necessary if either the 100 or 300 hz signals are the major contributors to the distribution or an amplification of greater than 2 is necessary if only the 800 hz signals contribute. This great an amplification is unlikely to be realized since guiding will not be complete nor will absorption be absent.

In fact, the distribution of bursts in figures 6c and 13 indicates that strong absorption is present at high magnetic latitudes on these L-shells. Accordingly, the source of the high L-value, high magnetic latitude steady noise must be near the position of the maximum occurrence rate.

Figures 6c and 13 also show that the source of the bursts at high L-values is near the equator. The common occurrence of bursts from the equator to 20° magnetic latitude at these L-values is in accord with the work of Liemohn (1967) and of Kennel and Thorne (1967) which showed that whistler mode signals can be amplified within about 20° of the equator.

In short, the source of steady signals at low L-values from 0000-0600 is near the equator whereas the source from 1800-2400 may lie between 0 and 30 degrees magnetic latitude. On the dayside at low L-values, the steady signals may be generated almost anywhere along a field line up to 40° magnetic latitude but at high L-values on the dayside the signals must be generated in the range 40 to 50 degrees. Finally the high L-value bursts must be generated near the magnetic equator.

We should mention at this point a source of bursts that is well understood. As noted in section 3, whistlers are included in the count of bursts. Whistlers are generated by lightning at the surface of the earth and occur at satellite altitudes only infrequently beyond the plasmapause (Carpenter, 1968). Under the influence of absorption and the inverse of

the focusing effect, mentioned above, as the whistlers travel upwards from the ionosphere towards the equator they should become progressively weaker and more difficult to detect. In those regions where whistlers are prevalent, this will result in a distribution of bursts with a maximum at the highest magnetic latitudes for which observations are made. Such distributions may be noted in the 1800-2400 LT interval in Figure 7 and in the 0600-1800 LT interval in Figure 13. It is probable that whistlers are principally responsible for these observations. While the distributions would give information concerning magnetospheric absorption if the burst populations were homogeneous, the admixture of at least two populations makes such calculations uncertain. In the present paper attention is directed primarily to bursts which originate in the magnetosphere.

One cannot expect that the above identification of source regions for the noise will lead to an unambiguous identification of the source mechanism without a detailed study of amplitudes, polarizations, and microstructure of the noise. However, we shall examine the mechanism used by Kennel and Petschek (1966) to determine the limit on stably trapped particle fluxes to see if it is consistent with our observations.

Kennel and Petschek, following the ideas of Sagdeev and Shafronov (1961) stated that doppler shifted cyclotron resonance of whistler mode waves with electrons greater than 40 kev in the equatorial regions would result in wave growth because

of the presence of a pitch angle anisotropy maintained by the loss cone. Besides providing a source for whistler mode noise in the magnetosphere this resonance gave an upper limit to stably trapped particle fluxes.

In this interaction, particles can either increase or decrease their pitch angles depending on the phase of the wave at the resonance. As electrons decrease in pitch angle, they give up some energy to the wave and as they increase in pitch angle they take energy from the wave (see for instance, Brice, 1964). Since there is a net flow of particles to lower pitch angles due to maintenance of the anisotropy by the loss cone, there is a net transfer of energy to the waves. The growth rate of the waves depends on the fractional number density of the resonant particles. There are more resonant particles at the equator because the resonant energy decreases as the magnetic field decreases and because the spectra of energetic particles in the magnetosphere are typically monotonically decreasing functions of energy. Therefore the mechanism should be dominant at the equator. In the remainder of this paper we shall refer to this mechanism of whistler mode wave growth and electron precipitation as the whistler mode loss cone instability.

The resonant frequency of 40 kev electrons with whistler mode waves lies in our passband in two regions of the magnetosphere. The first region is the outer region of the plasmasphere near the equator. If we assume a reasonable number density at L=4 of 500 particles/cm^3 the resonant

frequency at the equator is about 800 hz, but if we wish resonance at the same frequency at L=3 we require more than 5000 particles/cm^3. On the other hand, when the plasmapause extends to large radial distances, as occurs at extremely quiet times, the resonant frequency may lie well within our passband. For example, at L=6 for a density of 100 particles/cm^3 the resonant frequency is about 170 hz. However, at low L-values within the plasmasphere and at magnetic latitudes away from the equator the increased magnetic field results in a resonance frequency above our passband.

Outside the plasmasphere the reduced number density of thermal particles results in the resonance frequency with 40 kev electrons being above our passband. As we proceed to still higher L-values along the equator, however, we reach a second region starting about L=8 where the decreased magnetic field results in a lower resonant frequency. At L=8, if we have a number density of 1/cm^3, the resonant frequency with 40 kev electrons is again near 800 hz. At L=10 with a number density of 0.5 cm^{-3} the resonant frequency is 500 hz. As before, when we move off the equator the resonant frequency increases and goes above our passband.

As a candidate for explaining the steady noise, this mechanism may contribute to the low L-value noise in the equatorial region near the plasmapause boundary, but does not appear capable of providing all the steady noise within the plasmapause except perhaps from 0000-0600 LT, and it certainly does not provide the steady noise seen at high L-values and high magnetic latitudes.

However, the bursts of noise which occur at low magnetic latitudes and high L-values do coincide with the second region mentioned above, and as was mentioned in section 3 the center frequency of the bursts decreases with increasing L-values which would be expected from this resonance. A detailed study of this frequency shift will be postponed to a later paper, however. Thus we feel the whistler loss cone instability is the mechanism producing the bursts.

Since the bursts of noise we see are usually quite rapid, occurring within the rise time of our detector as shown in Figure 2d, we would expect that the resulting precipitation on the ground will not be a steady drizzle but will also occur in bursts. Such bursts of electron precipitation were first observed by Anderson and Milton (1964). They called them microbursts. The precipitated electrons were found to have an e-folding energy of from about 20 kev near L=6 (Anderson et al., 1966) to around 200 kev at L=8 (Venkatesan et al., 1968). These energies are near those expected in the whistler loss cone instability. Also, the microbursts occur mainly between the local times of 0600 and 1700 (Anderson et al., 1966). In fact, Oliven and Gurnett (1968) have shown a close association between chorus and microbursts, and since we have seen above that the high L-value bursts and chorus have similar local time distributions, it is not surprising that our bursts and microbursts have similar distributions. The importance of the correlation between our bursts and microbursts is that we

observe the bursts near the equator and decreasing in frequency of occurrence off the equator. This implies that the source of the precipitated electrons is the whistler loss cone instability acting at the equator, and that the source of the chorus is also the whistler loss cone instability, the strong bursts being partially guided by the field and reaching the ionosphere despite some absorption or perhaps propagating in ducts. The resulting chorus as observed at low altitudes will be then a superposition of bursts from many sources and we will not, in general, expect a one-to-one correlation between the microbursts and chorus bursts because the electrons are guided more closely than the bursts as Oliven and Gurnett (1968) state.

However, we might expect a one-to-one correlation to occur whenever Injun III was in a duct albeit with a certain time lag if the wave and particle were emitted the same direction. Since such a correlation was not found and since in the whistler loss cone instability the particles and waves travel in opposite directions, we have another supporting argument for the whistler loss cone instability.

In light of the above, we agree with the conjecture of Parks (1967) that microbursts are the result of a plasma instability which the above analysis indicates is probably the whistler loss cone instability. However, our data do not support the suggestion of Lampton (1967) that the instability occurs close to the earth. The small dispersion

of microbursts may result from the character of the wave particle interaction. As the wave propagates away from the equator it encounters progressively higher magnetic fields and therefore resonates with electrons of increasing energy. These electrons are injected into the loss cone later than the lower energy electrons and have to travel farther because the wave and the electrons are moving in opposite directions. Thus, the slower electrons have a head start both in time and distance and this may account for the fact that the faster electrons do not overtake the slow ones by more than a few milliseconds.

5. SUMMARY AND CONCLUSIONS:

Within the magnetosphere, in the frequency range from 10 hz to 800 hz, and above the OGO-3 spectrum analyzer thresholds, signals are observed commonly only in the range from 100-800 hz. Arbitrarily dividing these observed signals into steady noise and bursts results in two significantly different distributions both with respect to local time and L-value. For the steady noise we find the following:

1. Frequent occurrence near the equator at all local times for L-values less than 6.
2. Very weak magnetic latitude dependence for L-values less than 6 and for local times between 0600 and midnight.
3. Frequent occurrence only near the equator in the region below L=6 from 0000-0600.
4. Frequent occurrence above L=6 only at magnetic latitudes around 45° and only on the dayside.
5. Consistency with low altitude ELF hiss measurements.

6. The identification of the region above L=6 near magnetic latitudes of 45^{o} as a source of steady noise.

7. An inability to explain all the steady noise observed by the whistler loss cone instability alone.

For the bursts we find:

1. A contribution to the occurrence of bursts at low L-values from lightning-generated whistlers.

2. An increase in the frequency of occurrence at L-values above 7 for local times from 0400-1800.

3. A decrease in the frequency of occurrence of these high L-value bursts with increasing magnetic latitude.

4. Similarity in the region of frequent occurrence of these high L-value bursts, auroral microbursts and chorus.

5. Consistency between the region in which the whistler loss cone instability would generate signals in our passband and the observed region of high L-value bursts.

The latter four points imply that the whistler loss cone instability acting at the equator causes the auroral microbursts and the propagation of these bursts through ducts or by nonducted field guidance causes the chorus observed near the surface of the earth.

This study leaves unanswered several important characteristics of the signals for example, polarizations and amplitudes. These will be examined in later papers of this series. High time resolution studies of the microstructure of the bursts, however, will have to wait until the data from the search coil magnetometer on the OGO-5 satellite is examined.

6. ACKNOWLEDGMENTS:

We are pleased to acknowledge a number of helpful discussions with C. F. Kennel, J. M. Cornwall and F. Coroniti.

This paper represents one aspect of research done by the Jet Propulsion Laboratory for the National Aeronautics and Space Administration under NASA contract 7-100, GSFC-623-S-70-21. Financial support for the work at the University of California was provided by the Jet Propulsion Laboratory under contract 950403.

REFERENCES

Anderson, K.A., L.M. Chase, H.S. Hudson, M. Lampton, D.W. Milton, and G.K. Parks. Balloon and rocket observations of auroral zone microbursts. J. Geophys. Res., 71, 4617-4629, 1966.

Anderson, K.A., and D.W. Milton. Balloon observations of X-rays in the auroral zone 3. High time resolution studies. J. Geophys. Res., 69, 4457-4479, 1964.

Angerami, J.J. and D.L. Carpenter. Whistler studies of the plasmapause in the magnetosphere, 2. Electron density and total tube electron content near the knee in the magnetospheric ionization. J. Geophys. Res., 71, 711-725, 1966.

Brice, N. Fundamentals of very low frequency emission generation mechanisms. J. Geophys. Res., 69, 4515-4522, 1964.

Carpenter, D.L., F. Walter, R.E. Barrington, and D.J. McEwen. Alouette 1 and 2 observations of abrupt changes in whistler rate and of VLF noise variations at the plasmapause - A satellite-ground study. J. Geophys. Res., 73, 2929-2940, 1968.

Gurnett, D.A. and B.J. O'Brien. High-latitude geophysical studies with satellite Injun 3, part 5, Very-low-frequency (VLF) electromagnetic radiation. J. Geophys. Res., 69, 65-89, 1964.

Holzer, R.E., M.G. McLeod, and E.J. Smith. Preliminary results from the OGO-1 search coil magnetometer: Boundary positions and magnetic noise spectra. J. Geophys. Res., 71, 1481-1486, 1966.

Kennel, C.F. and H.E. Petschek. Limit on stably trapped particle fluxes. J. Geophys. Res., 71, 1-29, 1966.

Kennel, C.F. and R.M. Thorne. Unstable growth of unducted whistlers propagating at an angle to the geomagnetic field. J. Geophys. Res., 72, 871-878, 1967.

Lampton, M. Daytime observations of energetic auroral-zone electrons. J. Geophys. Res., 72, 5817-5823, 1967.

Liemohn, H.B. Cyclotron-resonance amplification of VLF and ULF whistlers. J. Geophys. Res., 72, 39-55, 1967.

Ludwig, G.H. The orbiting geophysical observatories. Space Science Rev. 2, 175-218, 1963.

Oliven, M.N. and D.A. Gurnett. Microburst phenomena 3. An association between microbursts and VLF chorus. J. Geophys. Res., 73, 2355-2362, 1968.

Parks, G.K. Spatial characteristics of auroral-zone X-ray microbursts. J. Geophys. Res., 72, 215-226, 1967.

Sagdeev, R.Z. and V.D. Shafronov. On the instability of a plasma with an anisotropic distribution of velocities in a magnetic field. Soviet Physics, JETP English Transl., 12 (1), 130-132, 1961.

Smith, E.J., R.E. Holzer, M.G. McLeod, and C.T. Russell. Magnetic noise in the magnetosheath in the frequency range 3-300 hz. J. Geophys. Res., 72, 4803-4813, 1967.

Taylor, W.W.L., and D.A. Gurnett. Morphology of VLF emissions observed with the Injun 3 satellite. J. Geophys. Res., 73, 5615-5626, 1968.

Thorne, R.M. and C.F. Kennel. Quasi-trapped VLF propagation in the outer magnetosphere. J. Geophys. Res., 72, 857-870, 1967.

Venkatesan, D., M.N. Oliven, P.J. Edwards, K.G. McCracken, and M. Steinbock. Microburst phenomena 1. Auroral zone X-rays. J. Geophys. Res., 73, 2333-2343, 1968.

TABLE 1

AMPLITUDES AND SPECTRAL POWER DENSITIES RESULTING IN 1 VOLT SIGNALS AT THE SPECTRUM ANALYZER OUTPUTS IN HIGH GAIN

FILTER CENTER FREQUENCY	AMPLITUDE OF TONE AT CENTER FREQUENCY	SPECTRAL POWER DENSITY IN BAND AROUND CENTER FREQUENCY	
		WHITE NOISE	PINK NOISE
hertz	mγ	γ^2/hz	γ^2/hz
10	37	1.8×10^{-4}	3.7×10^{-4}
30	13	6.0×10^{-6}	1.3×10^{-5}
100	3.2	2.2×10^{-7}	3.5×10^{-7}
300	2.6	3.7×10^{-8}	4.8×10^{-8}
800	2.2	1.8×10^{-8}	2.0×10^{-8}

FIGURE CAPTIONS

Figure 1a

The schematic diagram of the electronics associated with the search coil magnetometer.

Figure 1b

The voltage-frequency curves for various components shown in Figure 1a. The letters a, b, c, d refer to the components so labelled in the previous figure.

Figure 2

The raw outputs of the 15 spectrum analyzer channels plotted versus universal time in hours and minutes. For a discussion of scales etc. see text. a) Steady noise as observed while the satellite was inertially stabilized. b) Steady noise observed while the satellite was spin stabilized. c) Slow burst of noise obtained while the satellite was inertially stabilized.

Figure 2d

Rapid bursts of signal obtained while the satellite was spin stabilized. See text.

Figure 3

The local time - L-value distribution of steady noise occurring such that either the 100 or 300 hertz channel was above 1 volt or the 800 hertz channel was above 2 volts. The black shading represents those areas where such signals occurred over 50 percent of the time. The heavy dots cover the area where such signals occurred between 25 and 49 percent of the time and the light dots between 0 and 25 percent. Data taken above 30^{o} magnetic latitude were excluded.

Figure 4

The local time - L-value distribution of steady noise occurring such that either the 100, 300 or 800 hz channel was above 4 volts. The shadings and other comments of Figure 3 apply.

Figure 5

The local time - L-value distribution of bursts occurring such that either the 30, 100, 300 or 800 hz channel reached 2 volts. The shadings and other comments of Figure 3 apply.

Figure 6a

The magnetic latitude distribution of the percent occurrence of both bursts (black bars) and steady noise (cross-hatched bars) for each 10° range of magnetic latitudes in the two regions of local time and L-value as indicated on the figure. The threshold for detection of steady noise was 1 volt on the 100 or 300 hz channel or 2 volts on the 800 hz channel and of bursts was 2 volts on the 30, 100, 300 or 800 hz channel. Also shown are T, the total time in minutes spent in the range, N, the number of separate orbits from which the data were obtained and λ, the average magnetic latitude of these data.

Figure 6b

See comments of Figure 6a.

Figure 6c

See comments of Figure 6a.

Figure 6d

See comments of Figure 6a.

Figure 7

See comments of Figure 6a.

Figure 8

See comments of Figure 6a.

Figure 9

See comments of Figure 6a.

Figure 10

See comments of Figure 6a.

Figure 11

A meridional view of the day-time distribution of steady noise shown in figures 6a, b, c, d. The field lines shown represent the L-values obtained from a multipole expansion of the field and not the actual field lines of the magnetosphere. The black shading indicates where steady signals occurred greater than 50 percent of the time, the heavy dots between 35 and 49 percent, the light dots between 20 and 34 percent, and non-shaded areas between 0 and 19 percent.

Figure 12

A meridional view of the day-time distribution of steady noise similar to Figure 11 but for signals causing 4 volts on either the 100, 300 or 800 hz channel. The same shading scale as Figure 11 applies.

Figure 13

A meridional view of the day-time distribution of bursts of noise as shown by figures 6a, b, c, d. The same shading scale as Figure 11 applies.

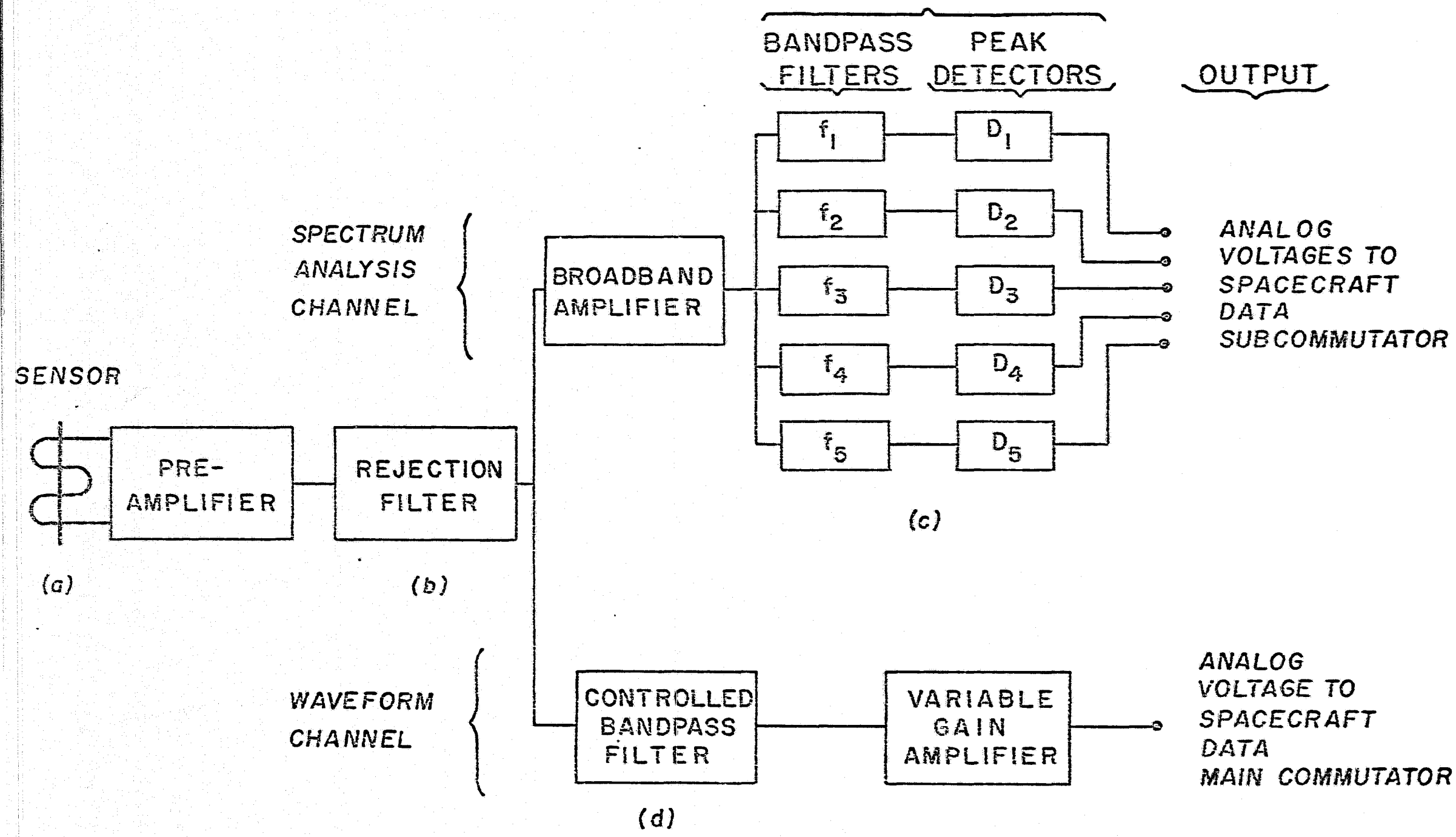
BANDPASS FILTERS
PEAK DETECTORS
OUTPUT
SPECTRUM ANALYSIS CHANNEL
BROADBAND AMPLIFIER
f_1
f_2
f_3
f_4
f_5
D_1
D_2
D_3
D_4
D_5
ANALOG VOLTAGES TO SPACECRAFT DATA SUBCOMMUTATOR
(c)
SENSOR
PRE-AMPLIFIER
REJECTION FILTER
(a)
(b)
WAVEFORM CHANNEL
CONTROLLED BANDPASS FILTER
VARIABLE GAIN AMPLIFIER
ANALOG VOLTAGE TO SPACECRAFT DATA MAIN COMMUTATOR
(d)

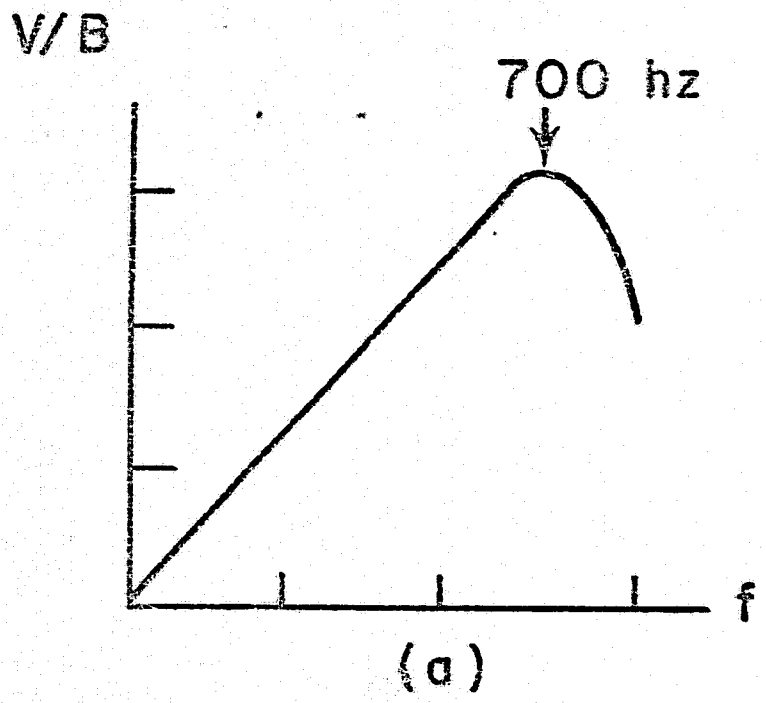
V/B
700 hz
f

(a)

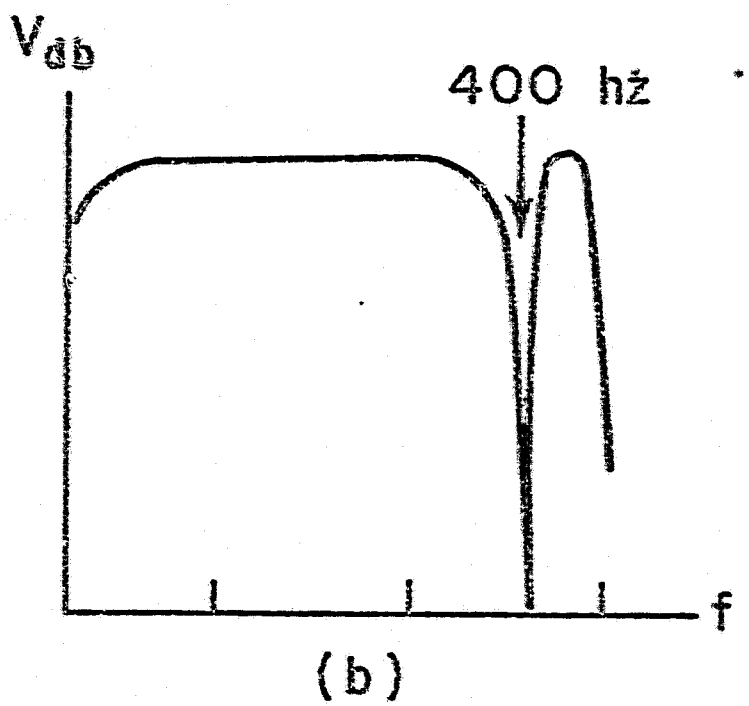
V_{db}
400 hz
f

(b)

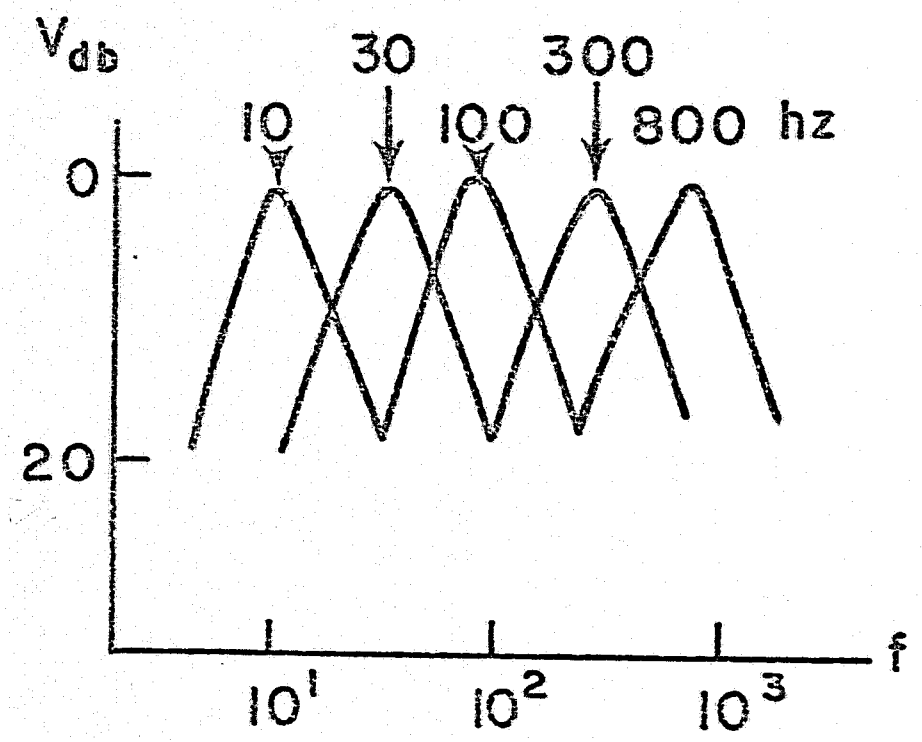
V_{db}
30
300
10
100
800 hz
0
20
f
10^1
10^2
10^3

(c)

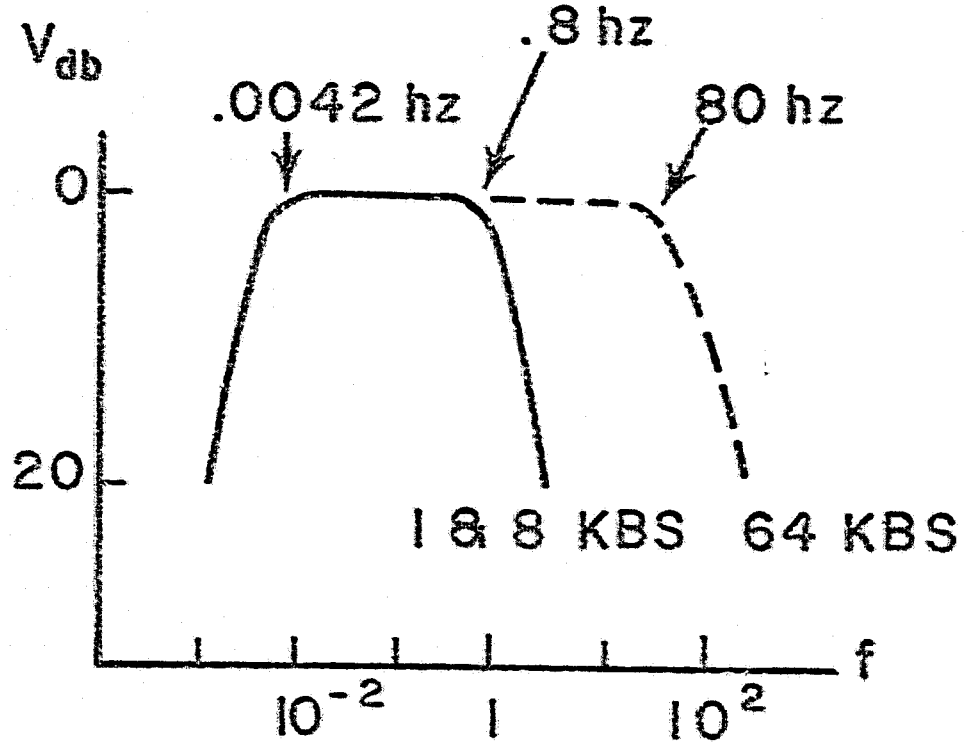
V_{db}
.8 hz
.0042 hz
80 hz
0
20
1 & 8 KBS
64 KBS
f
10^{-2}
1
10^2

(d)

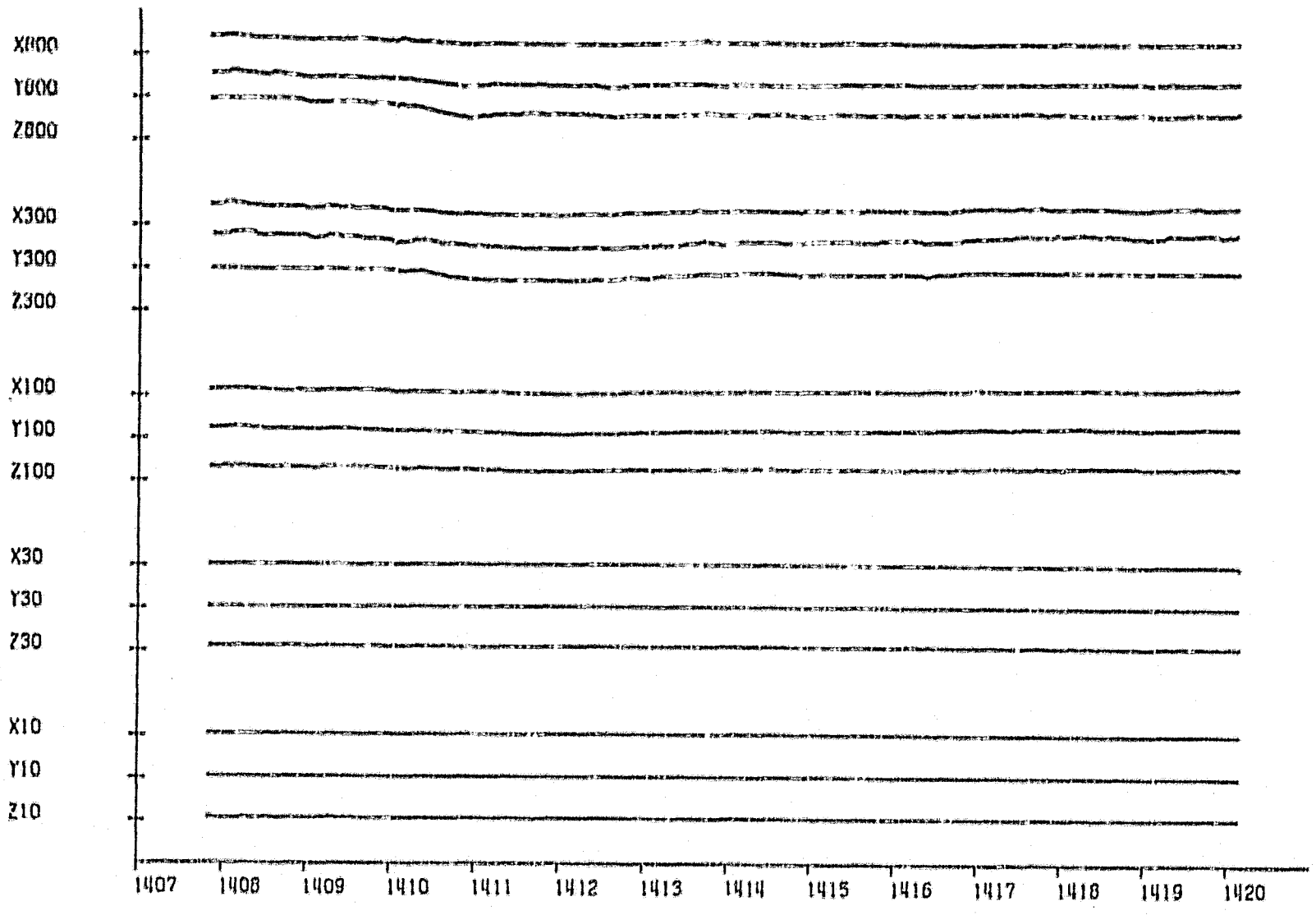

(a) 7/11/66

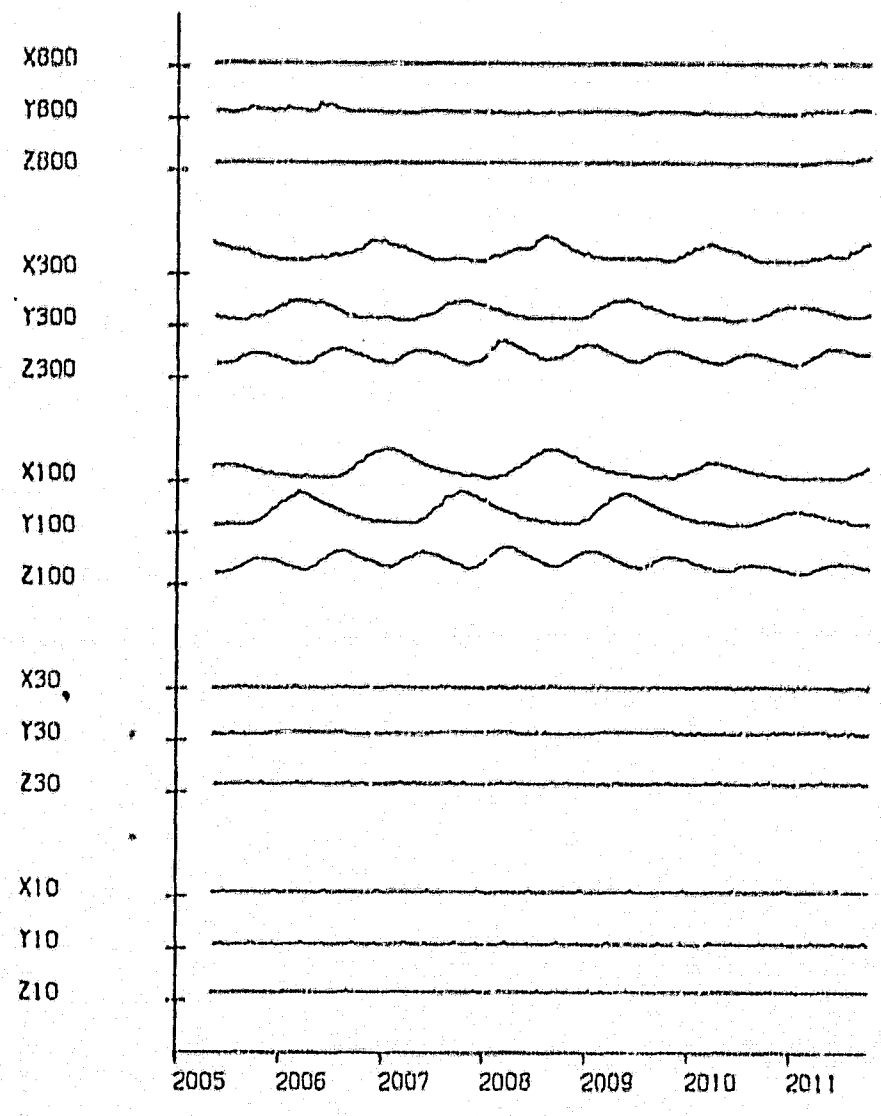

(b) 11/3/66

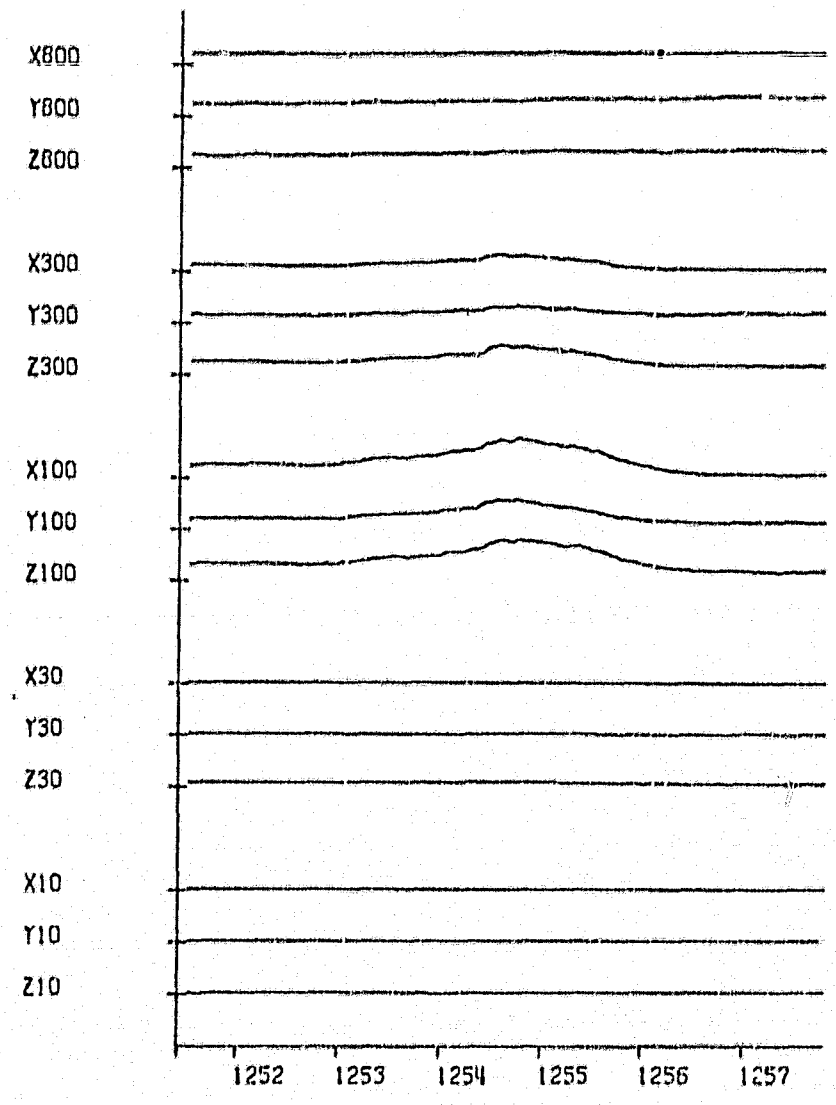

(c) 7/3/66

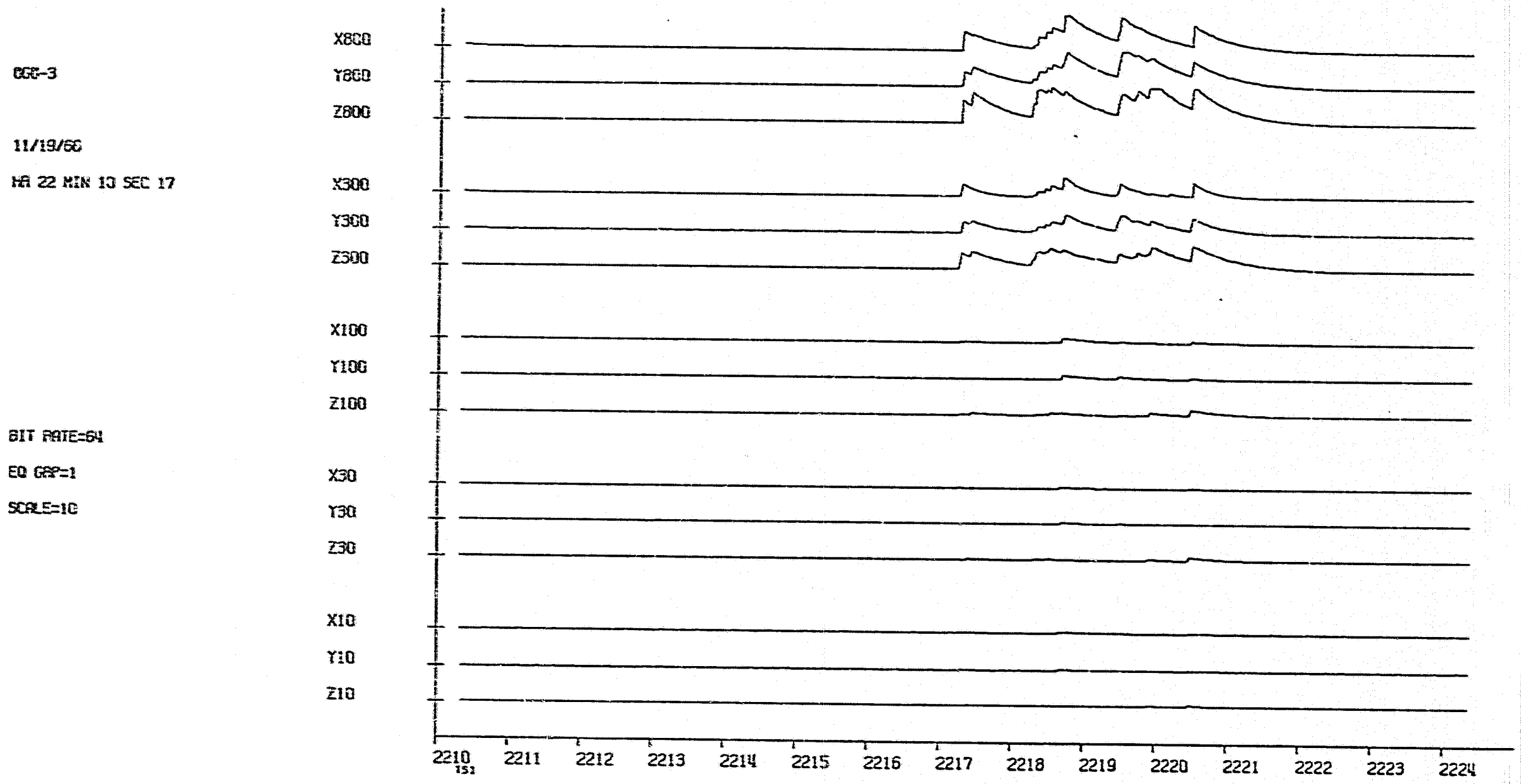
GGB-3
11/19/66
HR 22 MIN 10 SEC 17
BIT RATE=64
EQ GAP=1
SCALE=10
X800
Y800
Z800
X300
Y300
Z300
X100
Y100
Z100
X30
Y30
Z30
X10
Y10
Z10
2210
151
2211
2212
2213
2214
2215
2216
2217
2218
2219
2220
2221
2222
2223
2224

1800

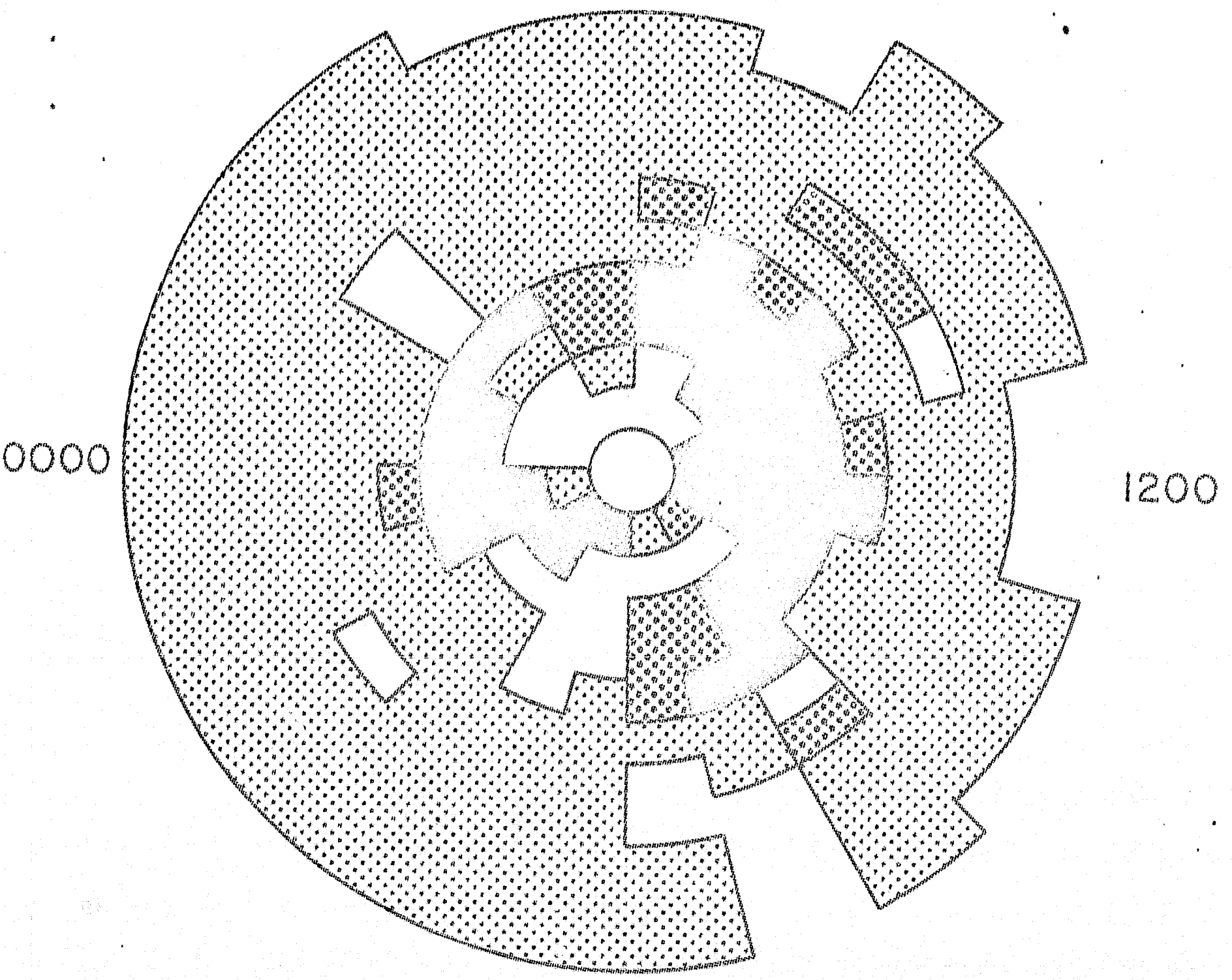

≥ 50 %

25-49 %

0-24 %

Insufficient Data

0 4 8 12

L-Value

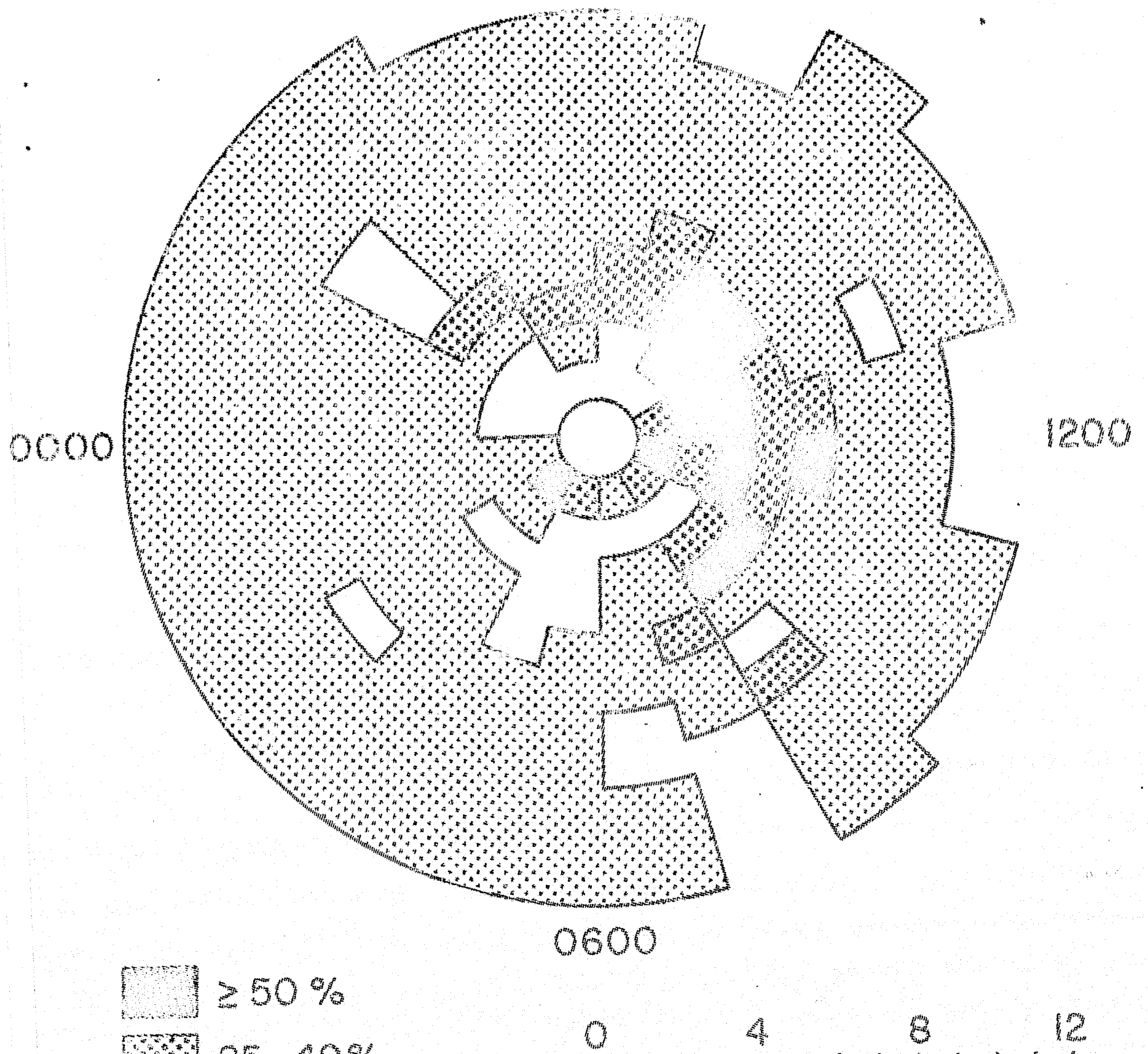
0000
1200
0600
≥ 50 %
25 - 49 %
0 - 24 %
Insufficient Data
0
4
8
12
L-Value

1200

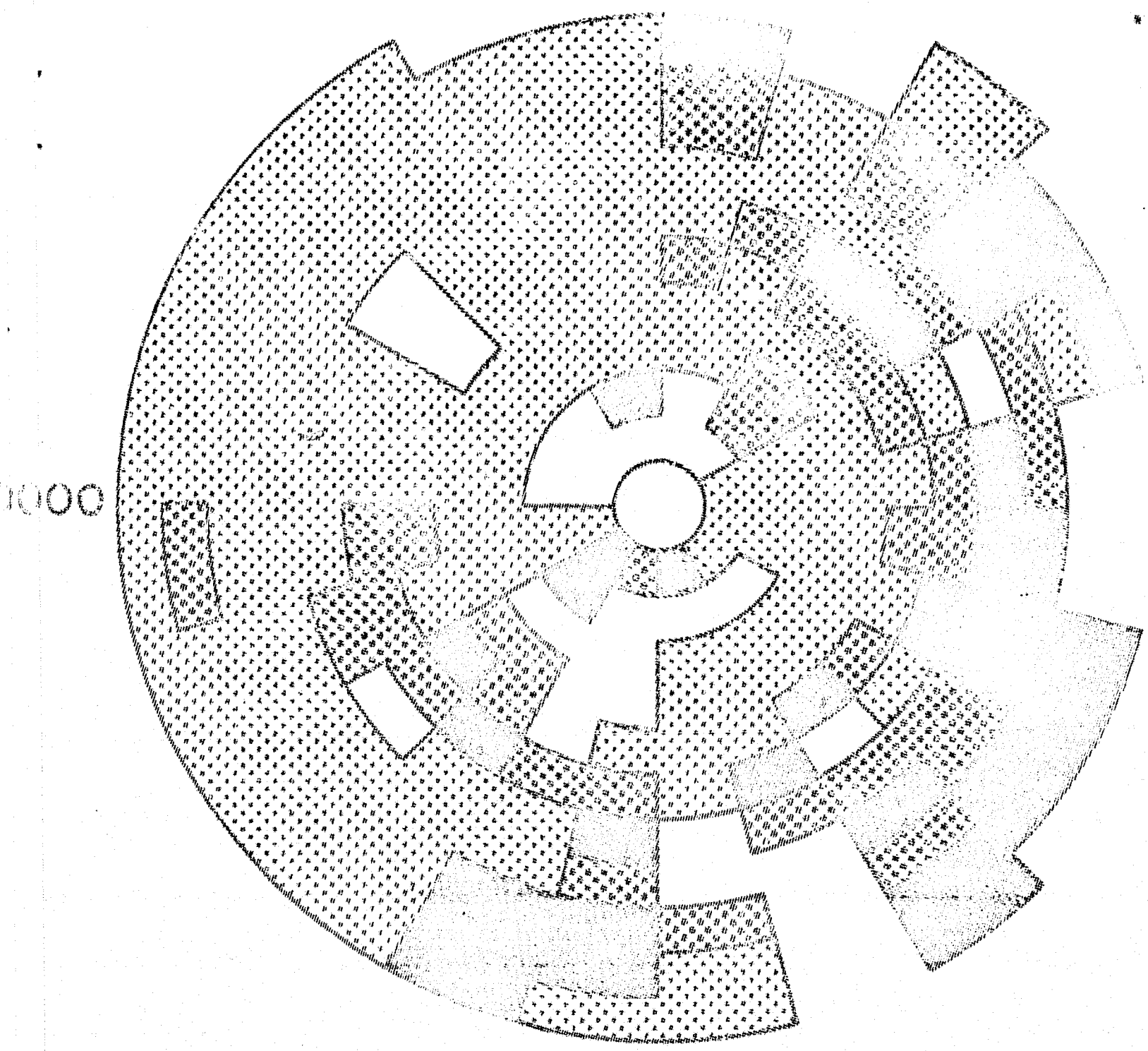

≥ 50 %

25-49 %

0-24 %

Insufficient Data

0 4 8 12

L-Value

0900 - 1800 LT

$2 \leq L < 4$

T	20	79	340	250	31
N	3	9	18	24	7
λ	7.9	17.0	24.4	34.4	42.6

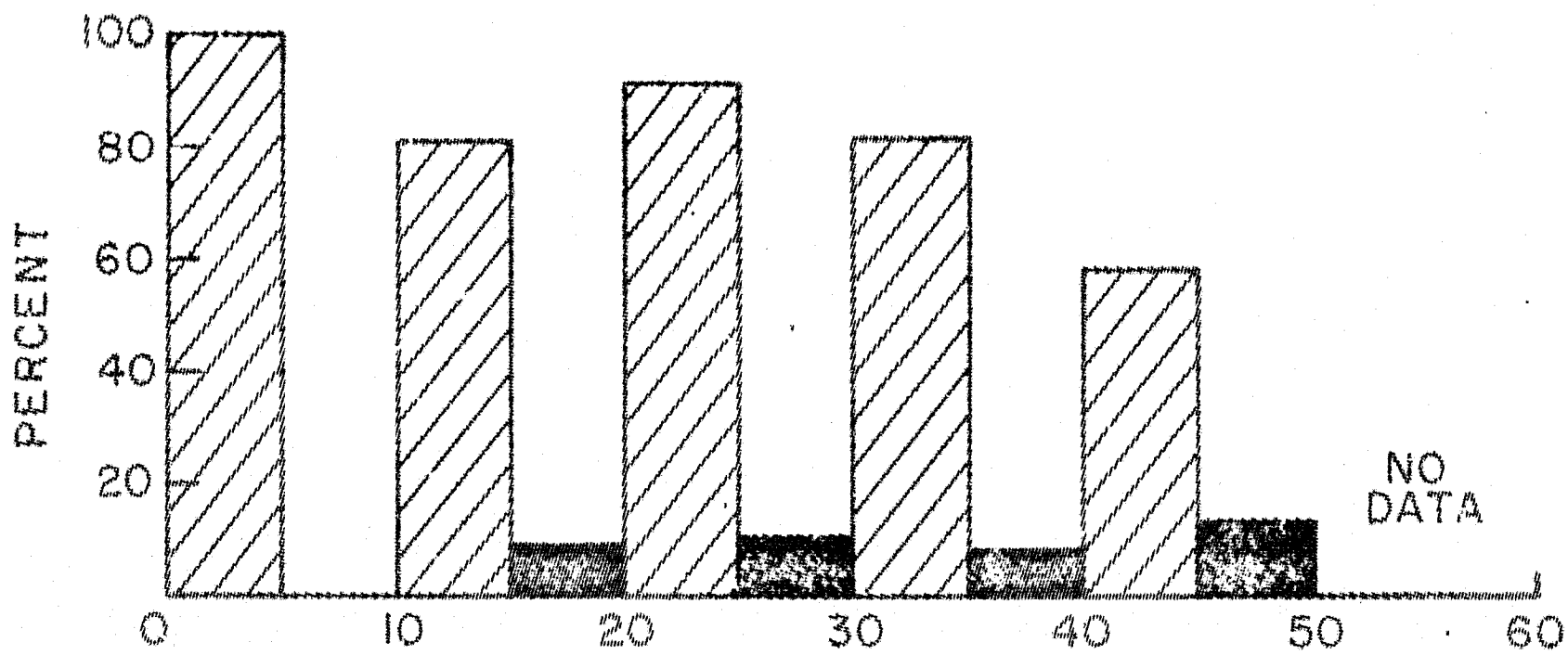

0900 - 1800 LT

$4 \leq L < 5$

T	116	203	194	115	100
N	9	12	17	13	16
λ	6.1	14.4	24.5	36.0	44.0

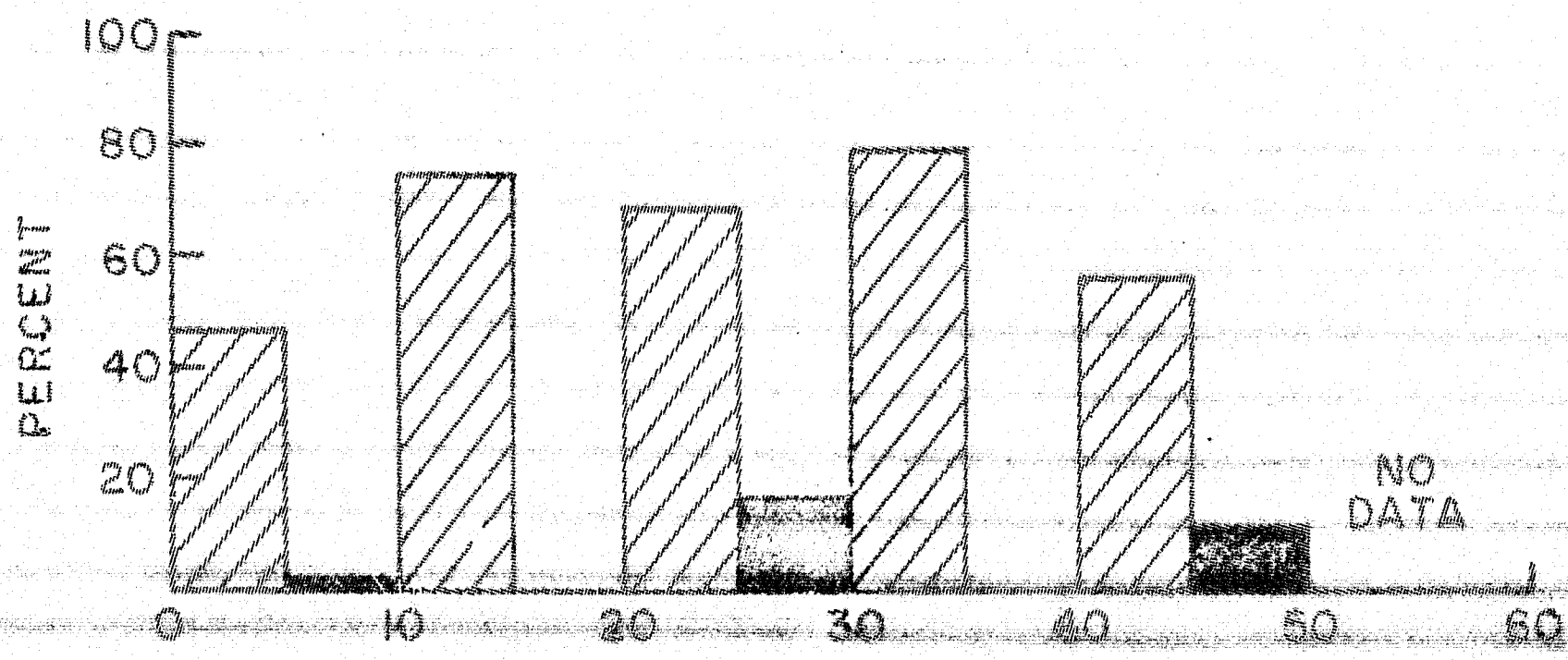

0900-1800 LT

$5 \leq L < 6$

T	301	216	351	107	100	23
N	18	15	20	12	9	7
λ	6.0	15.0	24.8	36.7	43.5	51.9

0300-1800 LT

$6 \leq L < 7$

T	383	267	334	90	58	7
N	18	10	17	7	5	3
λ	4.5	15.1	24.7	36.7	42.1	53.3

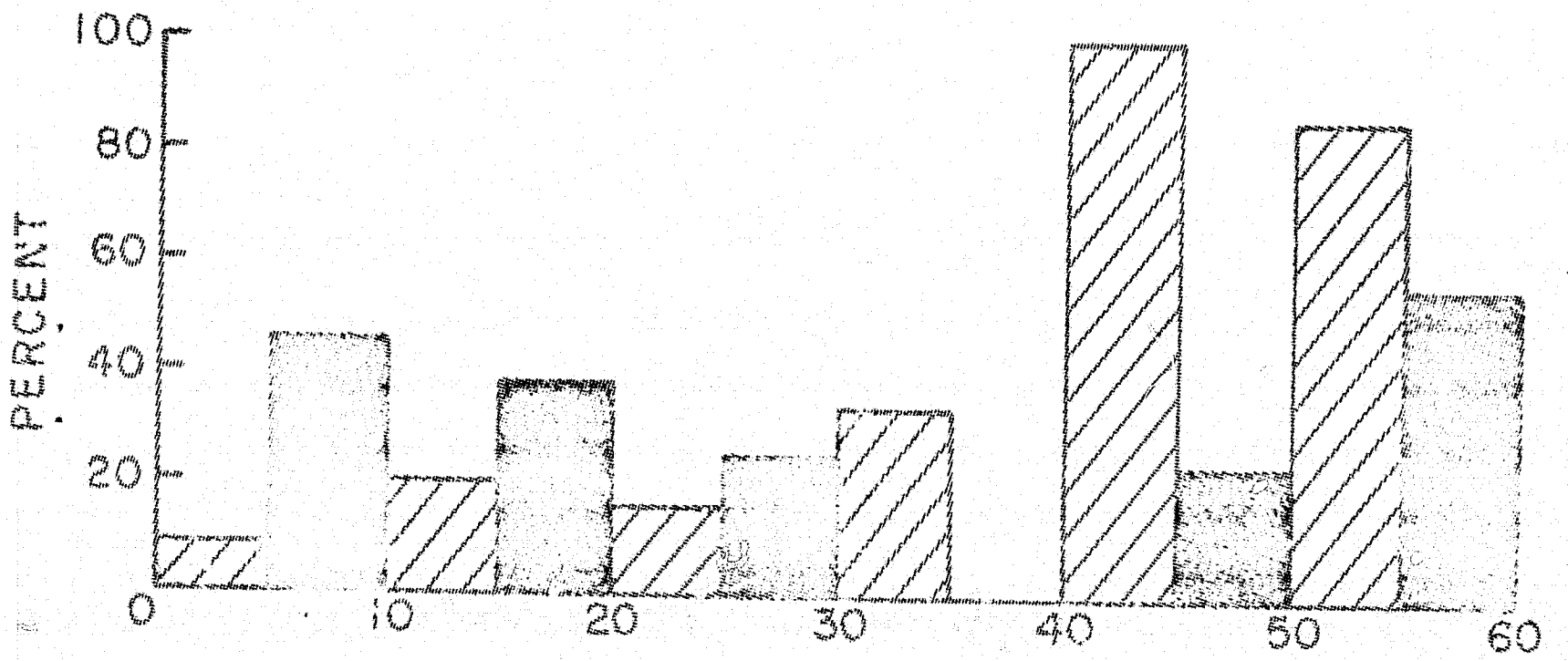

0900 - 1800 LT

$7 \leq L < 8$

T	496	285	248	100	69	12
N	19	10	12	7	6	2
λ	3.8	14.7	25.5	35.6	42.5	55.9

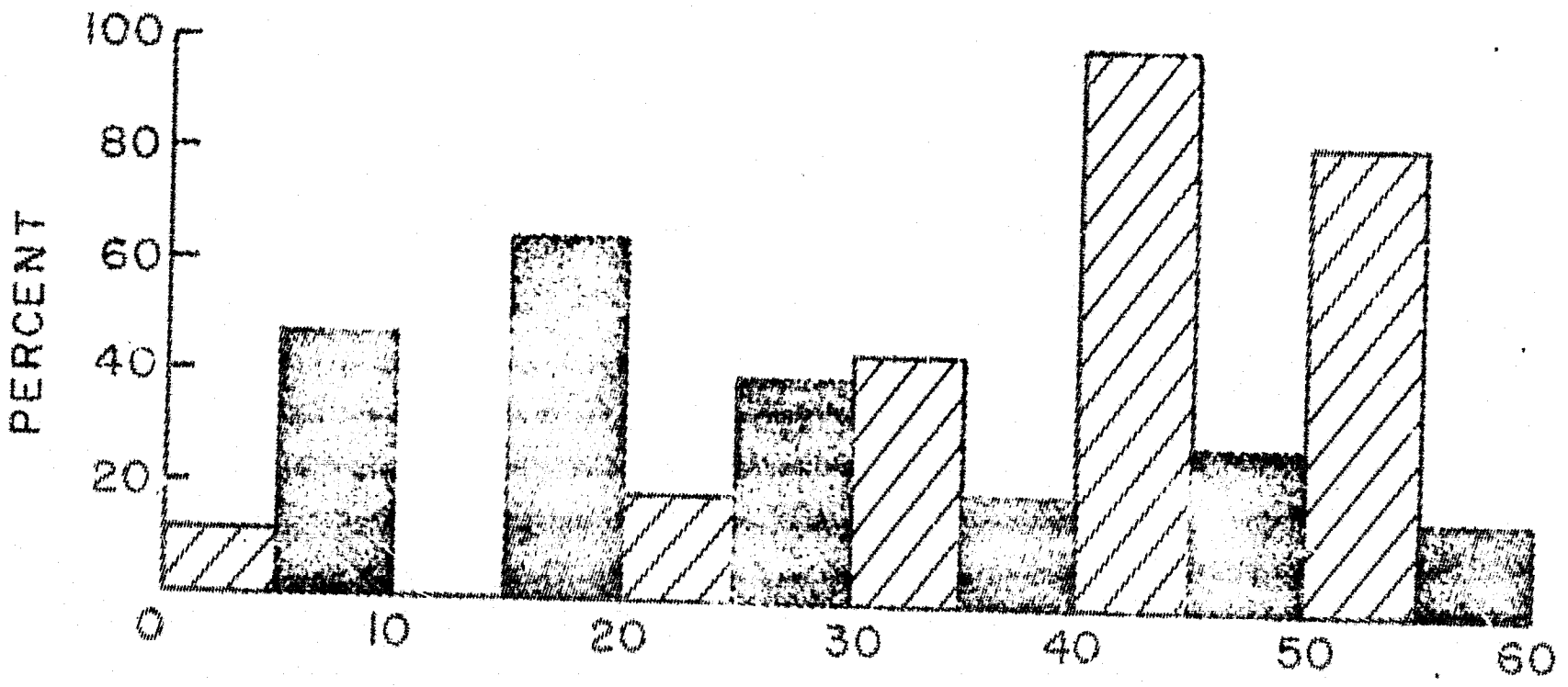

0900 - 1800 LT

$8 \leq L < 9$

T	541	125	269	81	53	17
N	20	6	11	7	7	4
λ	3.4	13.8	25.6	35.8	43.5	56.5

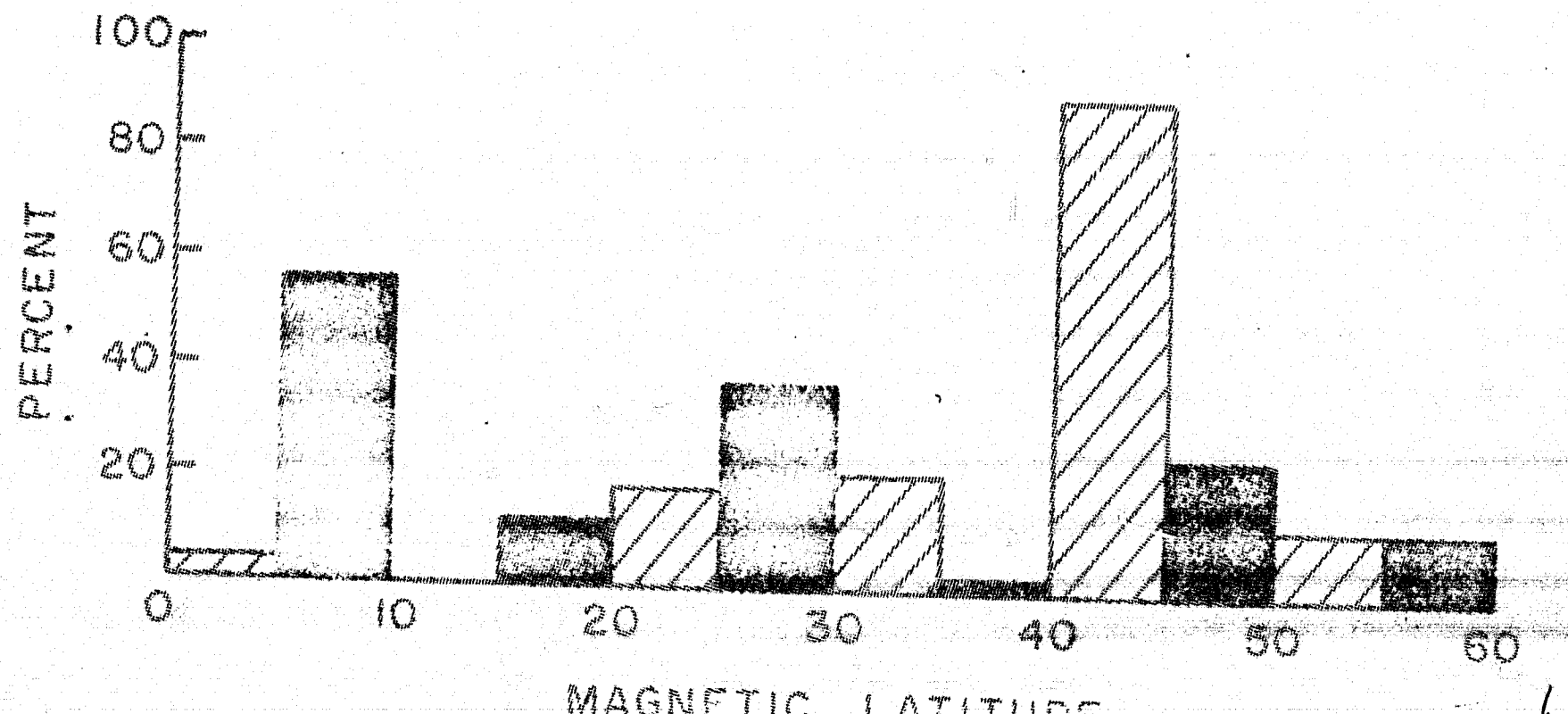

6c

0900 - 1800 LT

$9 \leq L < 10$

T	541	54	218	88	60	45
N	19	4	9	5	4	5
λ	4.3	12.1	24.3	36.9	44.9	55.1

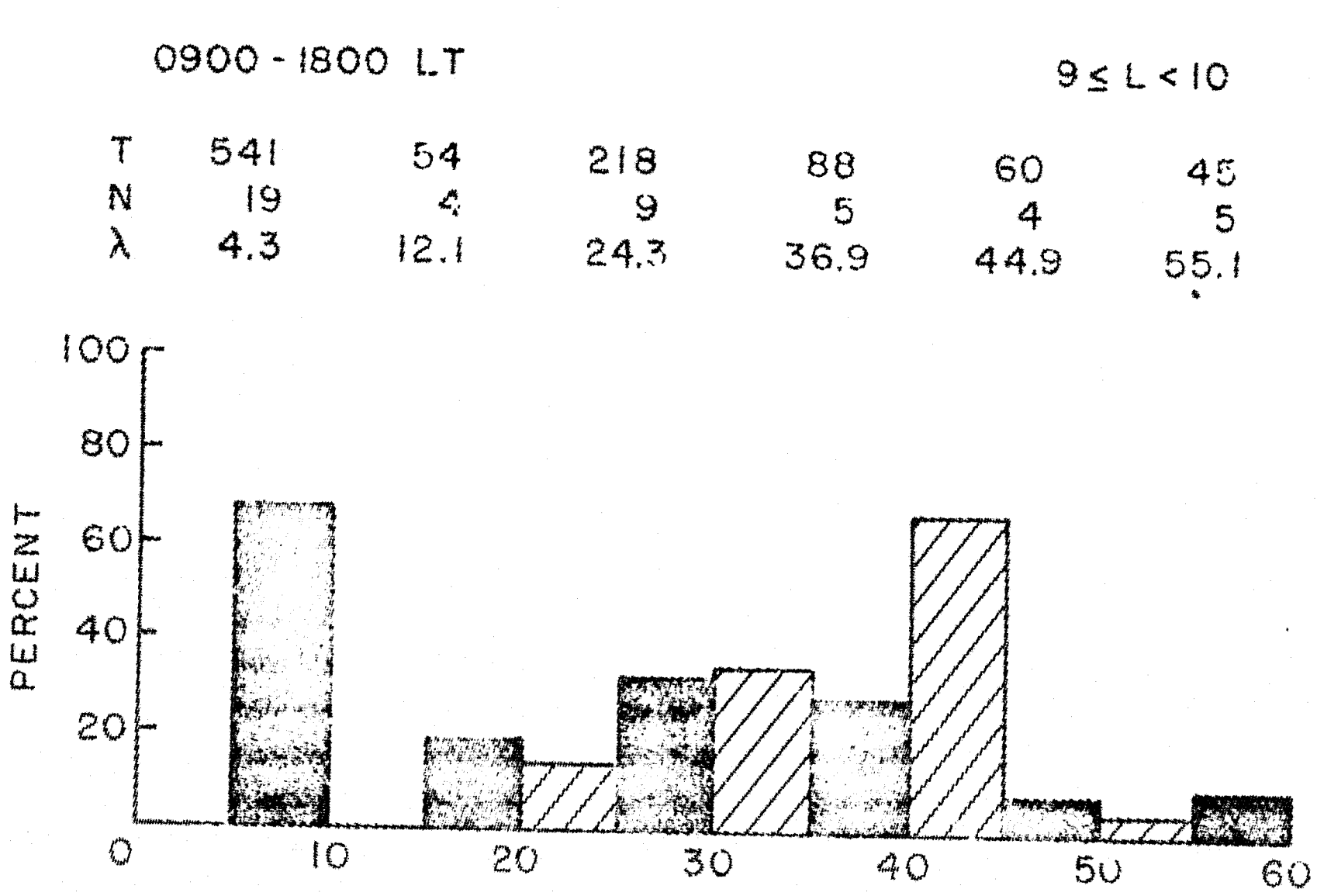

0900 - 1800 LT.

$10 \leq L < 12$

T	405	169	100	216	101	72
N	13	4	5	6	6	5
λ	4.6	14.4	24.1	35.5	46.1	54.8

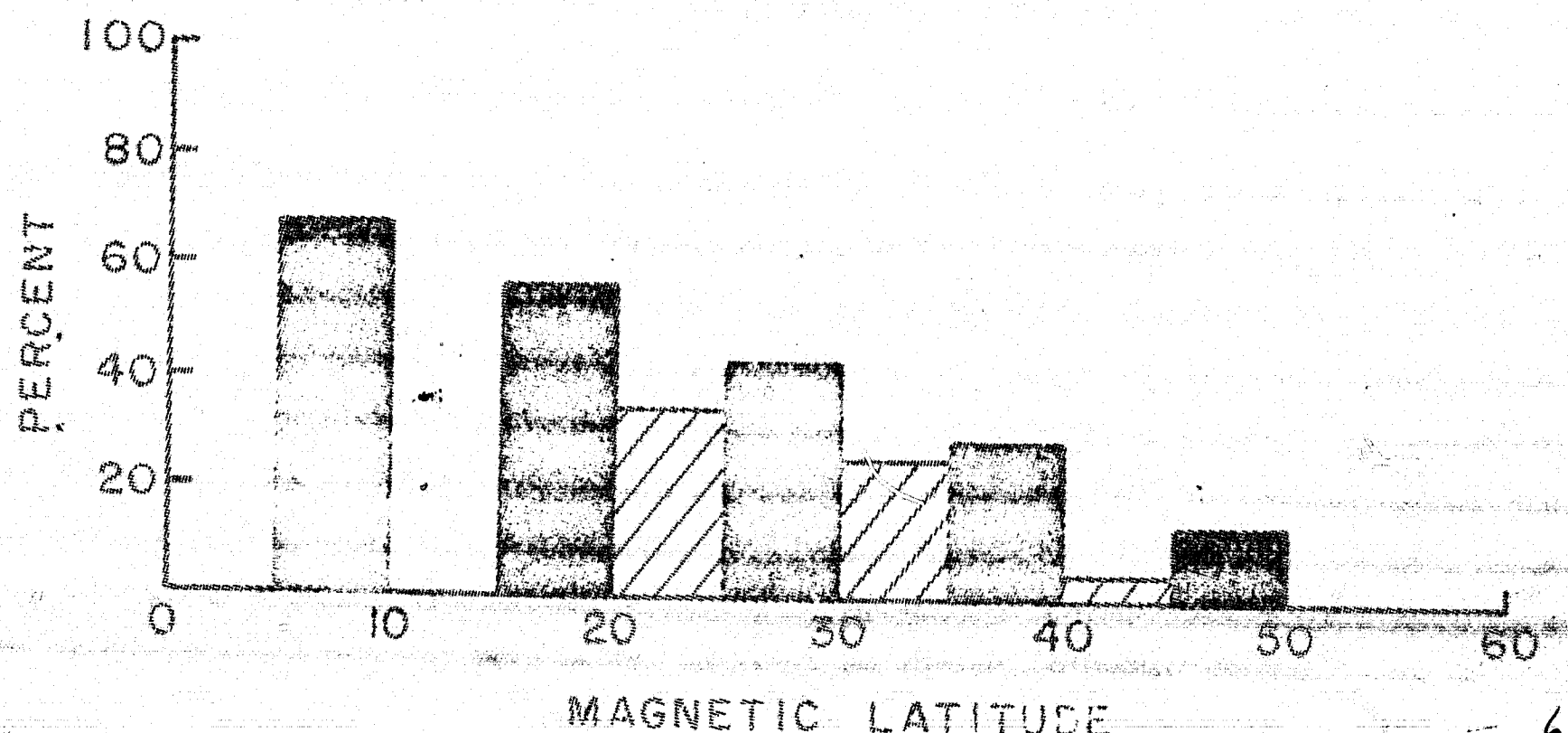

0000 - 0600 LT $2 \leq L < 6$

T	524	317	507	379	153	0
N	11	19	21	20	15	0
λ	4.7	15.9	24.8	34.5	45.1	

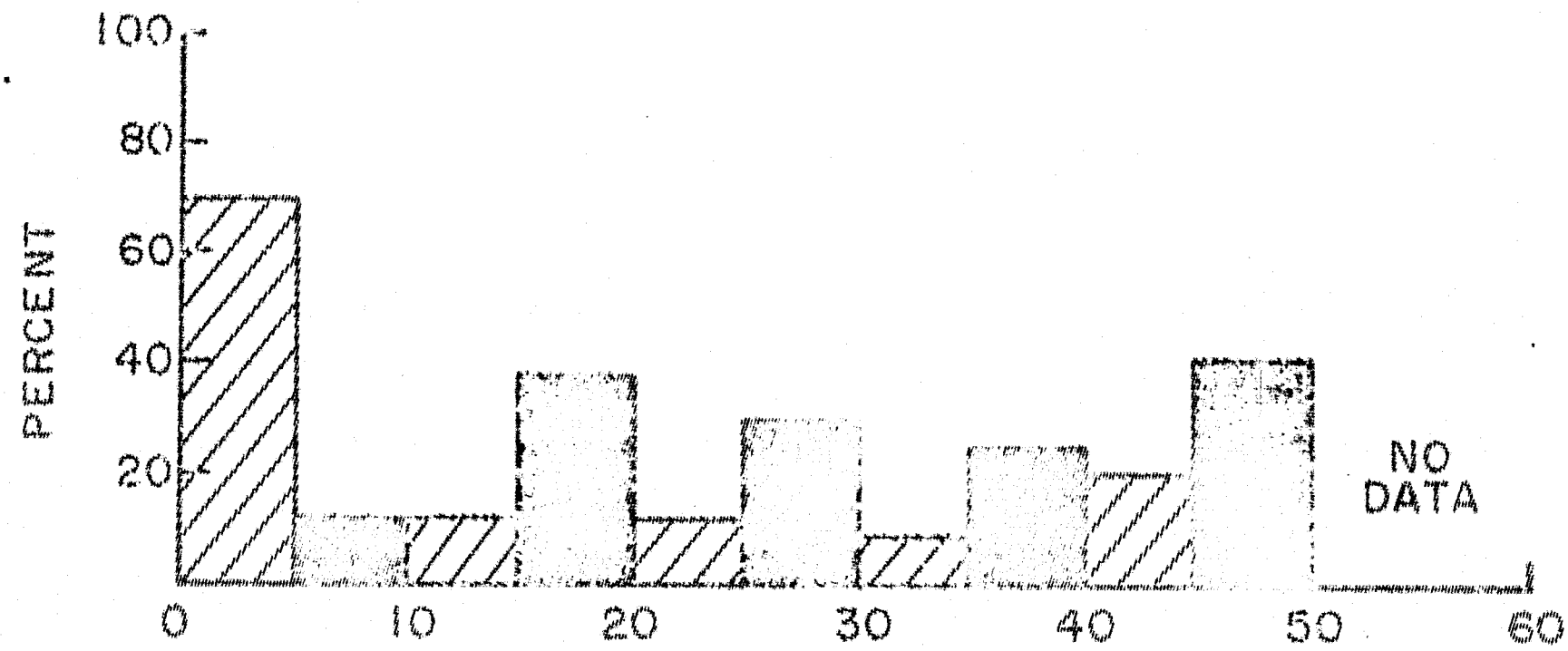

1800 - 2400 LT $2 \leq L < 6$

T	483	255	315	161	86	15
N	18	8	19	13	13	2
λ	3.8	15.3	23.5	34.5	45.3	50.8

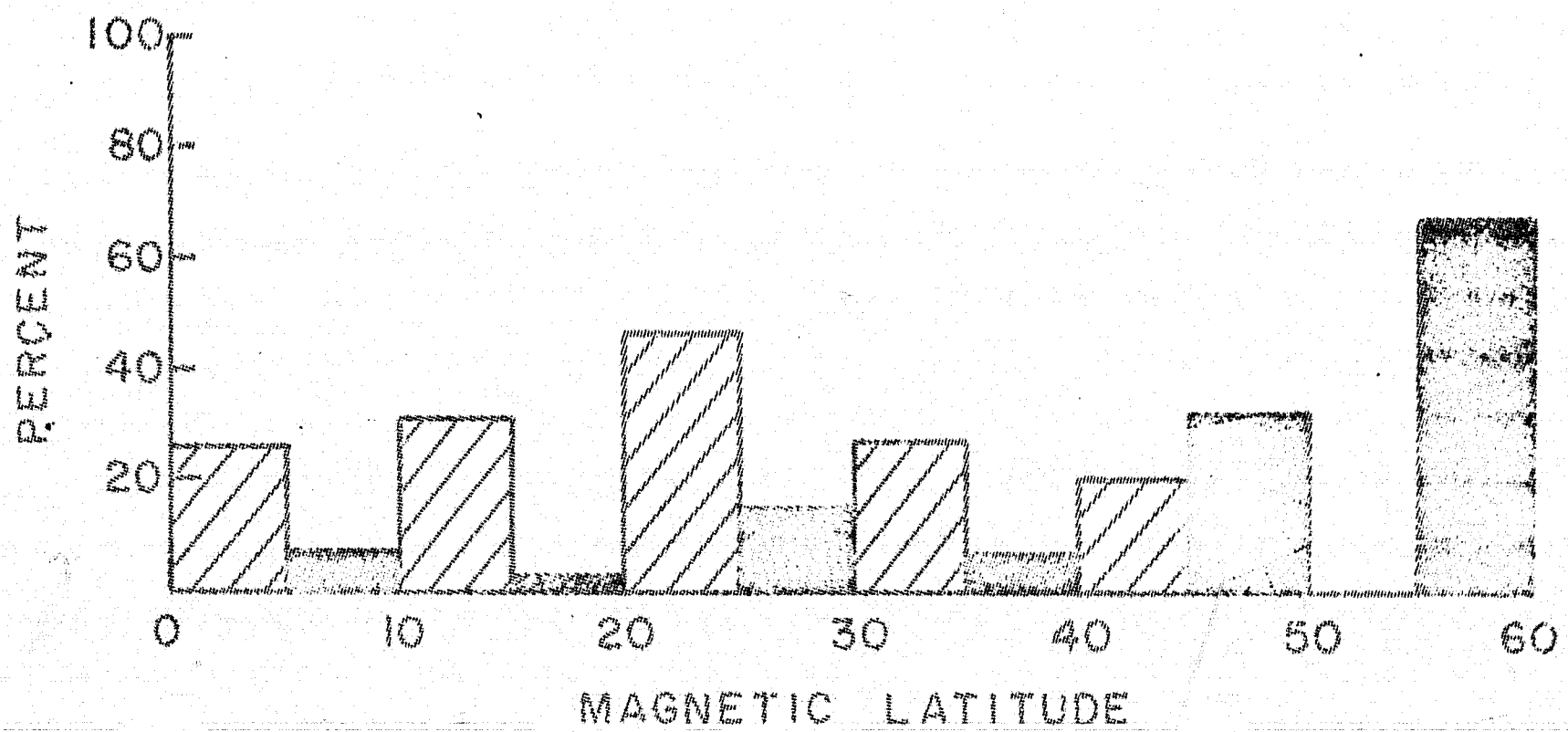

0000 - 0900 LT $6 \leq L < 8$

T	510	823	753	692	398	153
N	13	22	27	27	18	11
λ	6.8	14.0	26.5	34.4	44.3	53.1

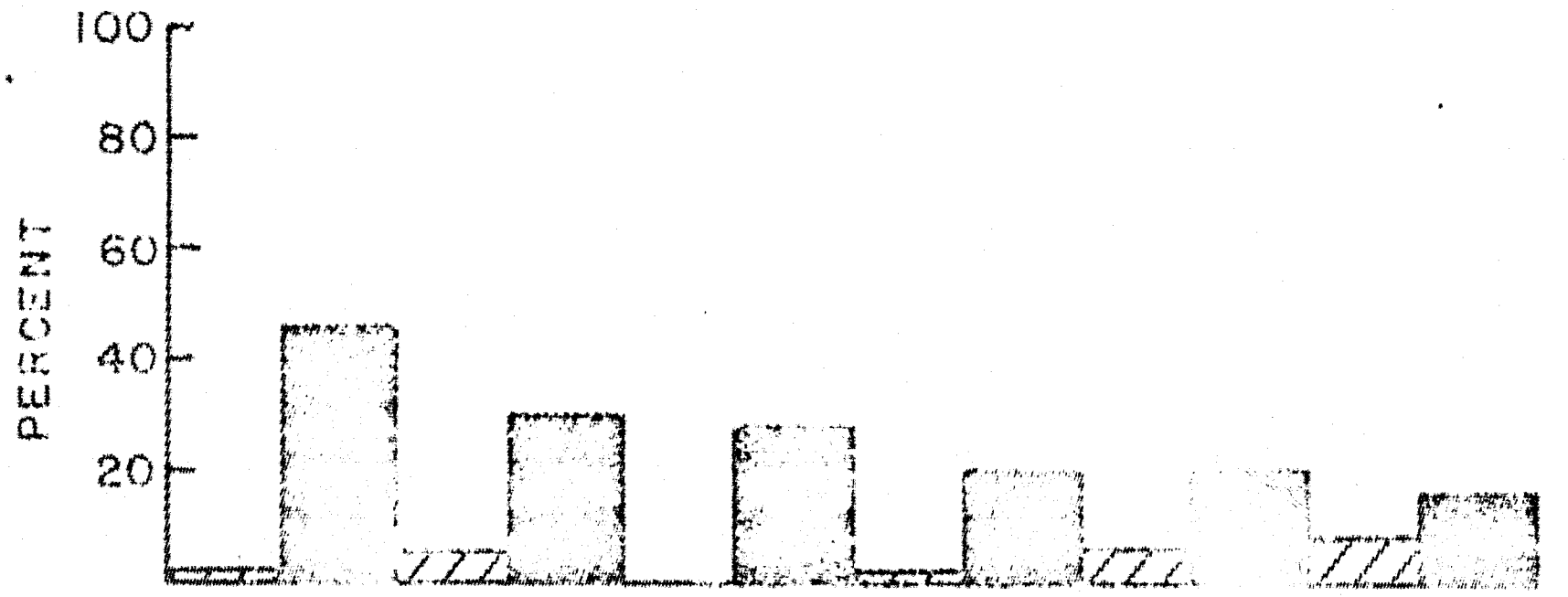

1800 - 2400 LT $6 \leq L < 8$

T	909	215	355	286	86	88
N	19	9	14	12	10	11
λ	5.8	12.1	23.5	33.4	45.8	52.3

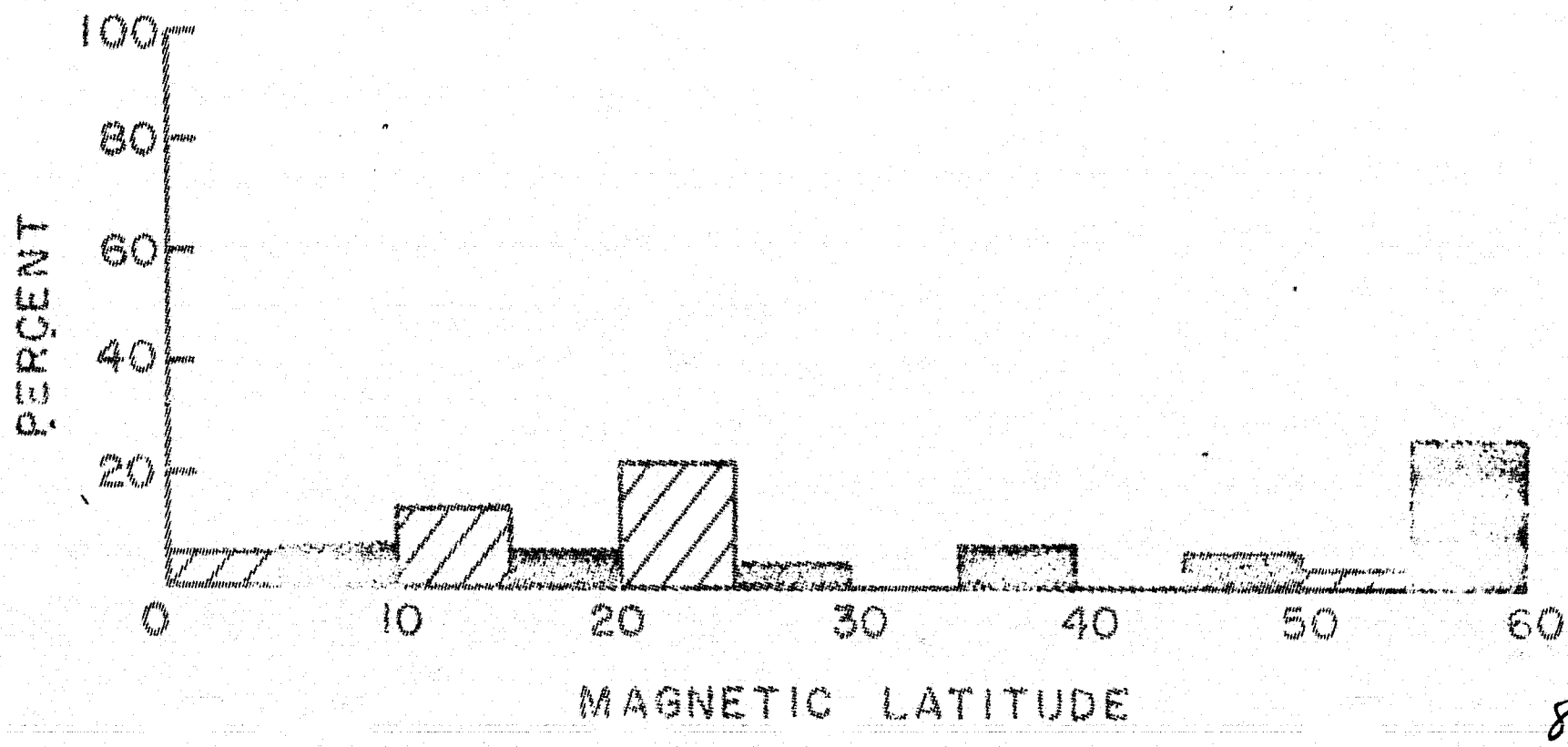

0000-0400 LT $8 \leq L < 12$

T	1502	734	1813	439	187	286
N	13	13	18	15	7	11
λ	5.0	14.7	24.5	33.1	45.3	53.0

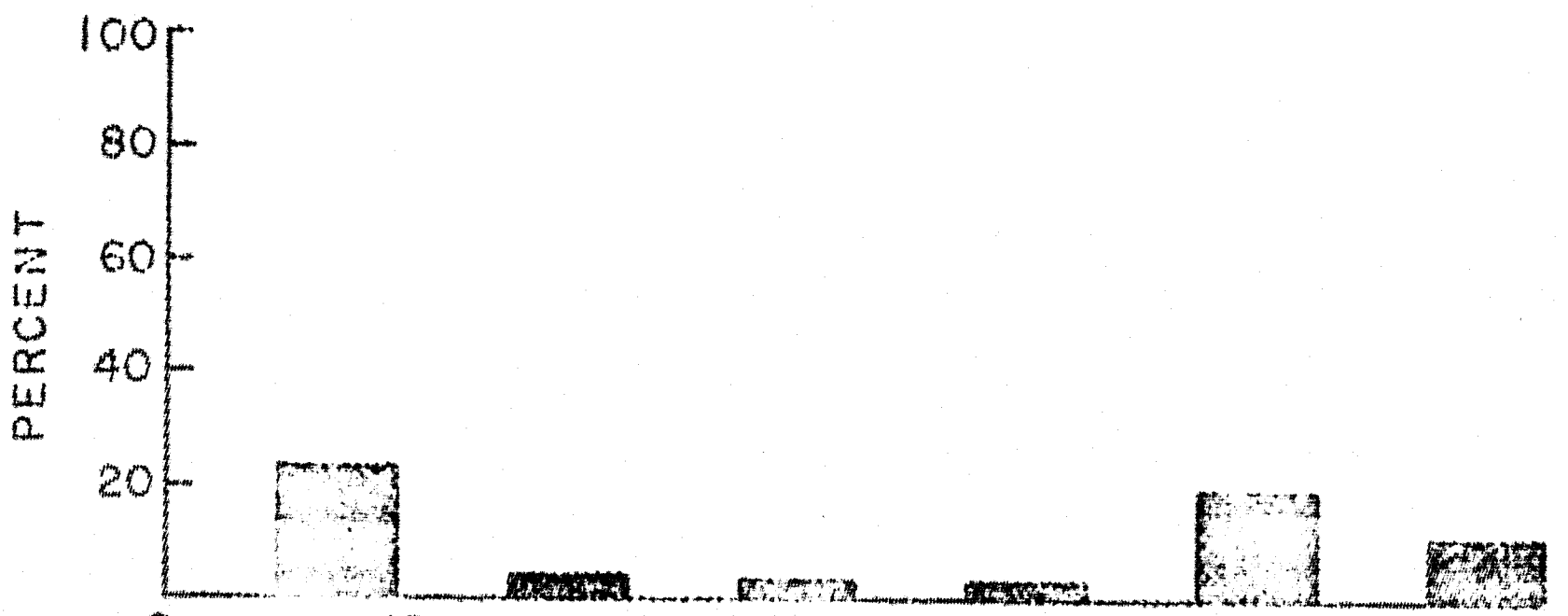

1800-2400 LT $8 \leq L < 12$

T	960	995	2215	1286	591	157
N	17	21	32	19	14	11
λ	5.6	14.6	24.8	34.6	44.3	53.7

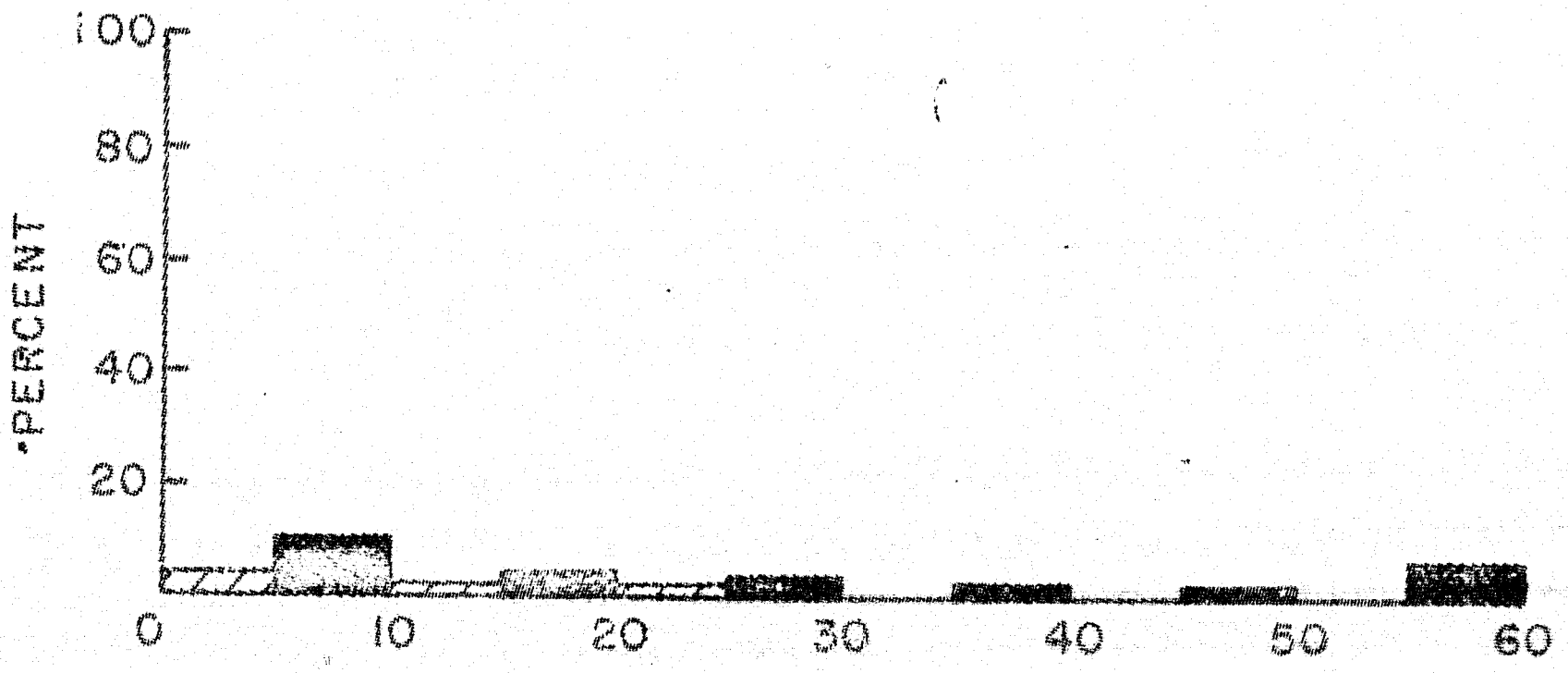

0600 - 0900 LT $2 \leq L < 6$

T	0	253	365	314	52	6
N	0	8	13	24	5	2
λ		15.3	25.0	34.3	44.6	52.2

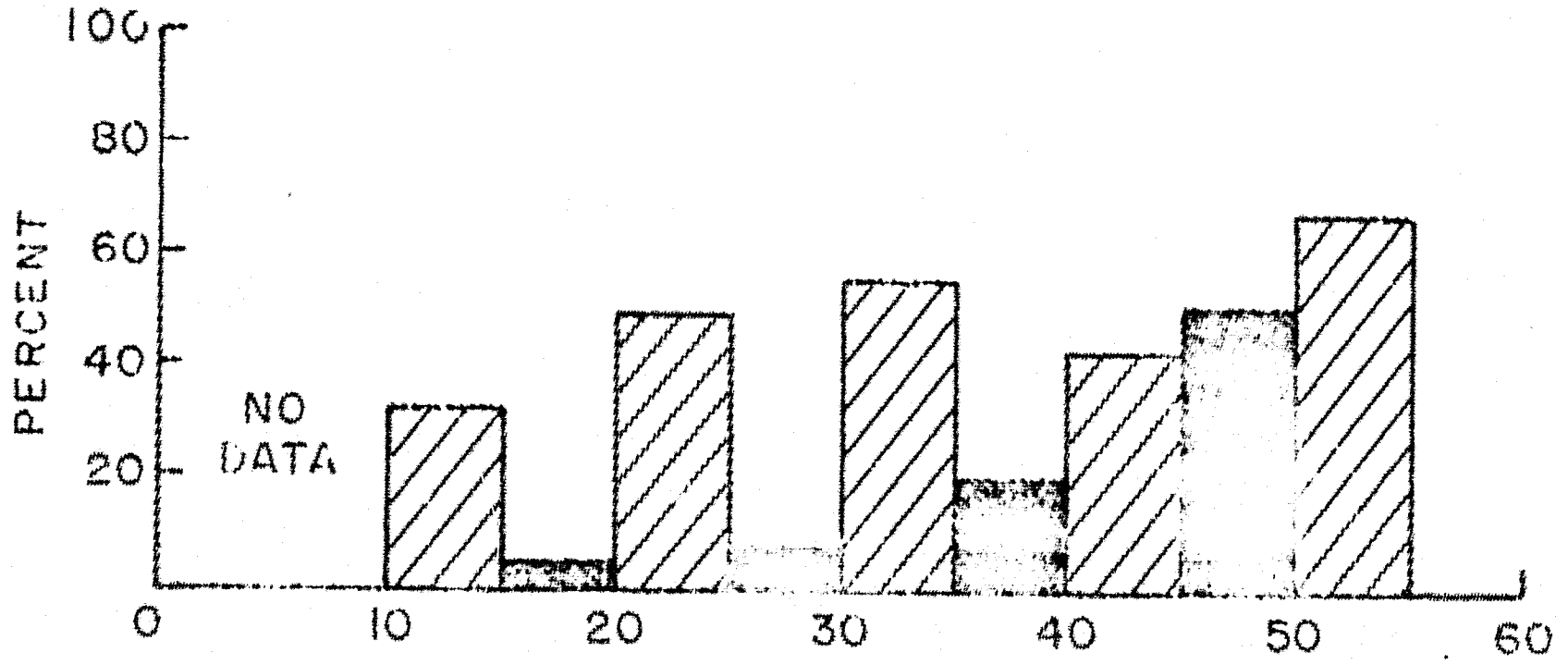

0400 - 0900 LT $8 \leq L < 12$

T	1858	228	785	320	106	124
N	18	8	14	11	4	5
λ	3.4	15.6	25.1	34.6	43.7	51.0

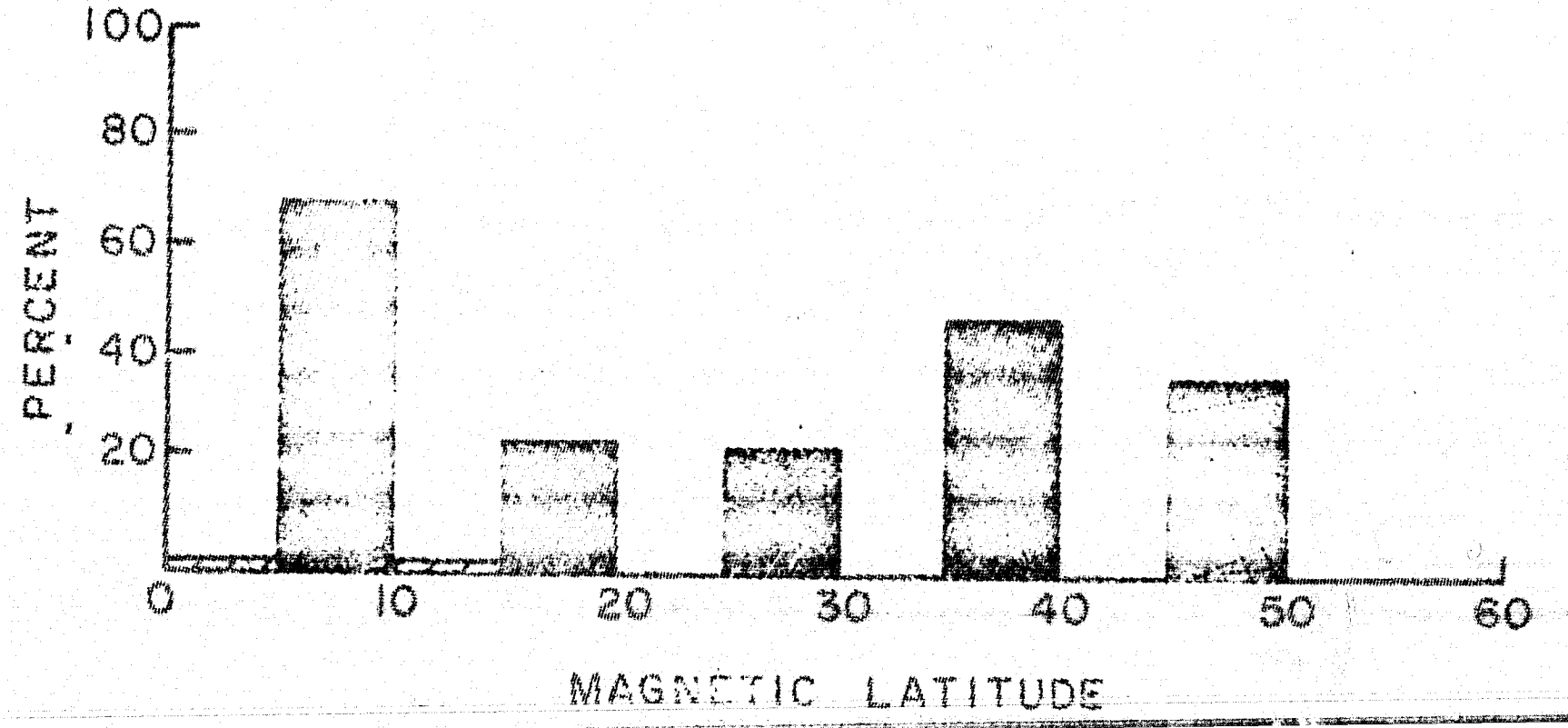

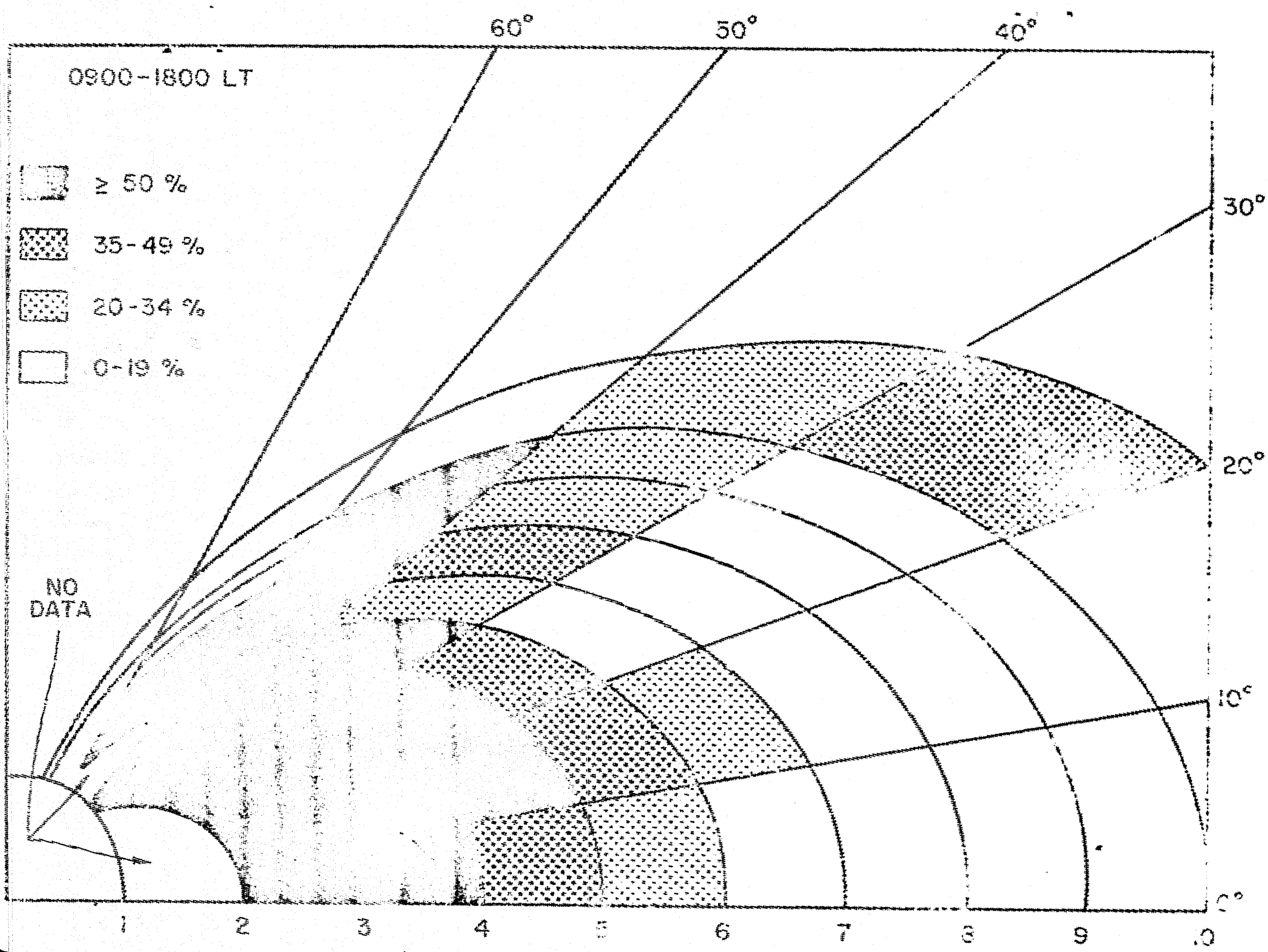
0900-1800 LT
≥ 50 %
35-49 %
20-34 %
0-19 %
NO DATA
60°
50°
40°
30°
20°
10°
0°
1
2
3
4
5
6
7
8
9
10

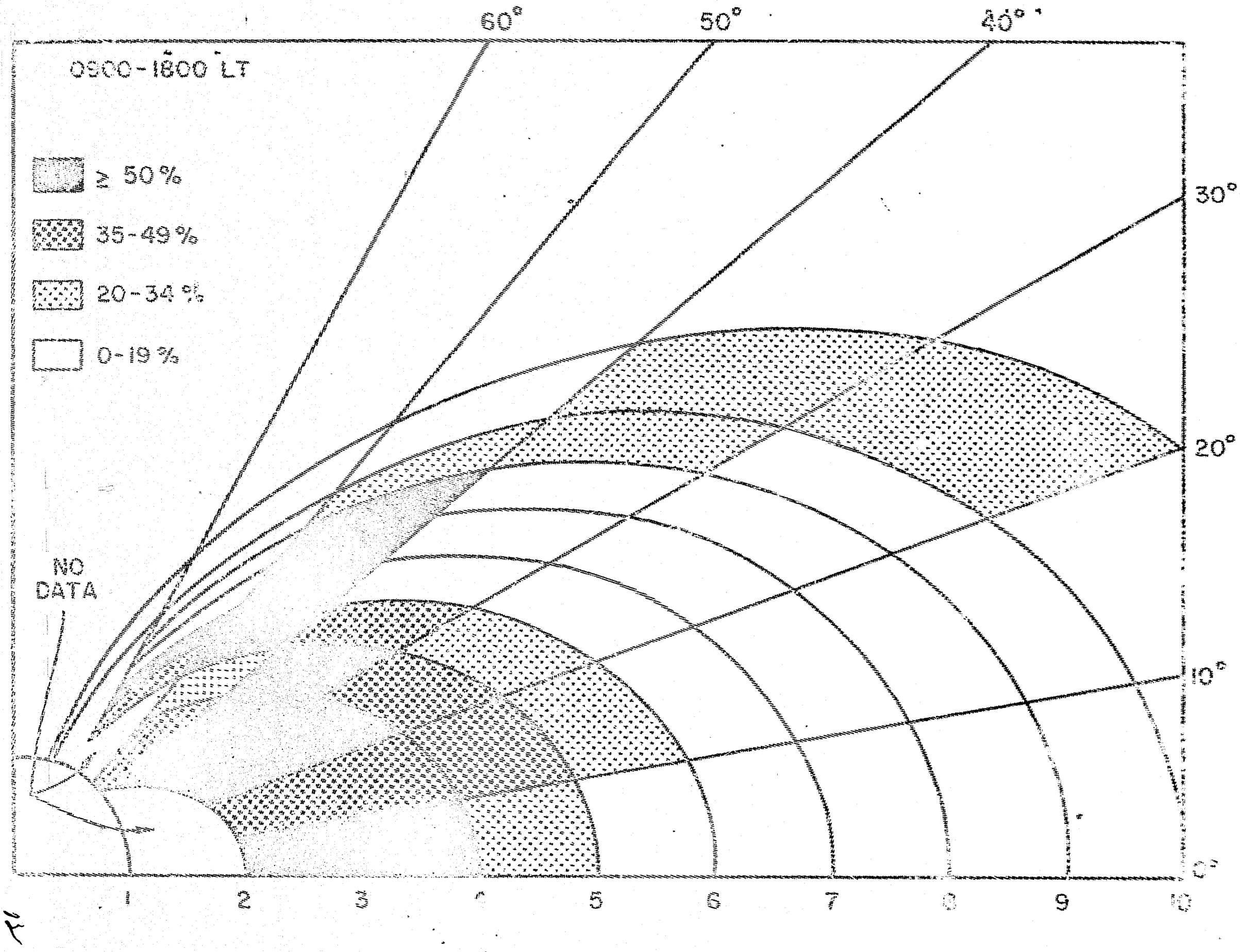
0900-1800 LT
≥ 50%
35-49%
20-34%
0-19%
NO DATA
60°
50°
40°
30°
20°
10°
0°
1
2
3
4
5
6
7
8
9
10

0800 - 1800 °LT

≥ 50 %

35 - 49 %

20 - 34 %

0 - 19 %

NO DATA

60°

50°

40°

30°

20°

1

2

3

4

5

6

7

8

9